Physica A 689 (2026) 131370

Contents lists available at ScienceDirect

Physica A

journal homepage: www.elsevier.com/locate/physa

Distributed-order fractional diffusion equation with Hilfer–Prabhakar fractional derivative

Wei Wang [a], Ralf Metzler [a,b], Živorad Tomovski [c,*]

[a] University of Potsdam, Institute of Physics and Astronomy, Potsdam-Golm, 14476, Germany
[b] Asia Pacific Centre for Theoretical Physics, Pohang, 37673, Republic of Korea
[c] Institute for Research and Application of Fuzzy Modeling, University of Ostrava, Brafova 7, Ostrava, 701 03, Czech Republic

ARTICLE INFO

Keywords:
Fractional diffusion equation
Anomalous diffusion
Hilfer–Prabhakar derivative
Ultraslow diffusion

ABSTRACT

Fractional diffusion equations (FDEs) are widely used to model anomalous diffusion in a variety of complex systems. In this work, we investigate a distributed-order FDE that incorporates the Hilfer–Prabhakar (HP) time-fractional derivative, which introduces a generalized memory kernel characterized by composite power-law scaling. This formulation extends the classical Riemann–Liouville (RL) and Caputo derivatives. We identify an admissible parameter regime under which the solution of the FDE behaves as a probability density function (PDF), and the HP derivative reduces to the Caputo-type under integer-order initial conditions. For the single-order case, we show that the PDF defined on an infinite domain can be expressed in terms of Fox H-functions in both short- and long-time limits, revealing distinctive subdiffusive behavior. Additionally, we derive asymptotic expressions for the mean squared displacement (MSD) corresponding to three representative order distributions: two-point, uniform, and beta. Notably, the uniform and beta distributions give rise to ultraslow diffusion. This study offers practical guidance for experimentalists seeking to apply FDEs with HP derivatives, emphasizing the importance of working within a physically consistent parameter regime. Our findings highlight the HP fractional framework as a powerful extension of classical FDEs, enabling a more versatile description of anomalous diffusion in systems with complex memory effects or trapping dynamics.

1. Introduction

Since Robert Brown's initial observation of the erratic motion of micron-sized particles expelled from pollen grains suspended in water [1], this phenomenon, now known as Brownian motion (BM), has been widely observed across various thermal systems and has played a foundational role in the development of statistical physics. A theoretical breakthrough came with Albert Einstein's landmark work [2], which offered a statistical interpretation and derived the diffusion equation describing BM:

$$\frac{\partial}{\partial t}P(x,t) = K_1 \frac{\partial^2}{\partial x^2}P(x,t). \tag{1}$$

where $P(x,t)$ is the probability density function (PDF) describing the likelihood of finding a particle at position x at time t, starting from the initial condition $P(x,0) = \delta(x)$ and K_1 is the diffusion coefficient. This formulation predicts that the solution is a PDF with Gaussian form and the mean-squared displacement (MSD) grows linearly over time, $\langle x^2(t)\rangle = 2K_1 t$.

* Corresponding author.
E-mail address: zhivorad.tomovski@osu.cz (Ž. Tomovski).

https://doi.org/10.1016/j.physa.2026.131370
Received 4 November 2025; Received in revised form 15 January 2026
Available online 24 February 2026
0378-4371/© 2026 Elsevier B.V. All rights are reserved, including those for text and data mining, AI training, and similar technologies.

Anomalous diffusion refers to a broad class of transport phenomena frequently encountered in biological, soft, and active matter systems [3–9], where particle dispersion deviates from the classical BM. Anomalous diffusion is typically characterized by a power-law scaling of the MSD [10–12]:

$$\left\langle x^2 \right\rangle = 2K_\mu t^\mu, \tag{2}$$

where the K_μ, with units of $\text{length}^2/\text{time}^\mu$, is the generalized diffusion coefficient and μ is the anomalous diffusion exponent. When $0 < \mu < 1$, the process is called subdiffusion, often arising from trapping, crowding, or obstructed environments. When $\mu > 1$, it is known as superdiffusion, typically driven by long-range correlations or rare, large jumps. Normal diffusion is recovered when $\mu = 1$, and ballistic motion corresponds to $\mu = 2$.

Several models have been developed to effectively describe anomalous diffusion in various systems. One prominent framework is the continuous time random walk (CTRW), with scale-free waiting time densities $\psi(t) \simeq t^{-1-\mu}$ with $0 < \mu < 1$ and jump length densities with finite variance [11,13–22].[1] To analytically describe the nonlocal and memory effects inherent in such systems, the concept fractional derivatives, has emerged as a powerful mathematical tool, finding applications across physics and engineering [22–31]. A key development connecting CTRWs with fractional differential equations was made by Hilfer and collaborators, who introduced a master equation incorporating the Riemann–Liouville (RL) fractional derivative within the general CTRW framework [15]. Another significant advancement in this area was made by Schneider and Wyss [32], who generalized the classical diffusion equation (1) into a fractional diffusion equation (FDE) by incorporating RL-derivative, which is mathematically equivalent to Caputo derivative under appropriate initial conditions [33,34]. They also derived closed-form solutions to the FDE using Fox H-functions [31]. FDEs can be derived as the continuum limit of CTRWs and in the context of FDEs with RL or Caputo type, the relaxation of modes follows the Mittag–Leffler pattern [35] that interpolates between an initial stretched exponential and a long-time inverse power-law. When external potentials influence the particle dynamics, the FDE framework can be extended to the fractional Fokker–Planck equation [11,16,36]. For instance, a constant external force introduces drift (advection) terms into the dynamics. These drift effects manifest in various physical systems, such as transient currents in amorphous semiconductors under electric fields [37], fluid transport in porous media subject to temperature and pressure gradients [38], anomalous motion in gel electrophoresis [39], and hydrodynamic dispersion in flow fields [40].

For most physical applications, the Caputo derivative is often favored due to its compatibility with standard initial conditions, which can be directly applied in modeling. However, the RL-derivative remains essential for theoretical investigations, as it imposes less stringent requirements on the differentiable properties of the function. In order to interpolate between the RL and Caputo fractional derivatives, the Hilfer fractional derivative [41–43] was proposed by introducing an type parameter $\nu \in [0, 1]$, which controls the "mix" between the RL and Caputo derivative. The Hilfer derivative provides modeling flexibility by allowing a continuous transition between RL and Caputo forms. This is especially useful when the nature of the memory effects or the proper initial conditions for a system are not clearly defined. The Hilfer-time fractional derivative has been used in the analysis of fractional diffusion equations, obtaining that such models may be employed in the context of glass relaxation and aquifer problems [44–47]. Another important generalization is the Prabhakar fractional derivative [48,49], which extends the RL and Caputo frameworks by replacing the power-law memory kernel in the RL integral with a generalized Mittag–Leffler function [50]. Depending on the order of differentiation and the corresponding integral, the Prabhakar derivative can also be formulated in RL-type and Caputo-type versions.

As a possible generalization of single-order FDEs, distributed-order FDE, in which the fractional order derivatives are integrated over a distribution of orders, was first proposed and studied in Refs. [51,52]. This approach is particularly well-suited for describing systems with a non-unique diffusion exponent, addressing two key motivations: one is single-particle tracking experiments, revealing that intracellular transport is highly heterogeneous, and indicating that a single diffusion exponent may be insufficient [53–56]; the second fold is that deviations of the MSD from the power-law (2) may be observed, e.g., ultraslow diffusion [57], which can be also observed in annealed CTRWs with logarithmic waiting time distribution [58,59], in cooling granular gases [60,61] and Sinai diffusion in quenched random landscapes [62–65]. The idea for the ordinary type differential equations with distributed order derivatives was first proposed in the works by Caputo [66] for generalizing the stress–strain relation of inelastic media. A basic framework for the numerical solution of distributed order differential equations was introduced in Ref [67]. Recently, in [68–70] the solution of generalized distributed-order diffusion-wave equations with composite time-fractional derivative was studied.

In this paper, we propose a generalized distributed-order FDE with Hilfer–Prabhakar (HP) time-fractional derivative, referred to as the HP-FDE. The HP derivative, which unifies the Hilfer and Prabhakar formulations, has previously been employed in classical equations of applied mathematics, including the heat equation and the free electron laser equation [71,72]. It is worthy noting that RL and Caputo derivatives generate pure power-law memory kernels, and the Hilfer derivative interpolates between them, whereas the HP derivative incorporates a tempered kernel with multi-scale memory via the generalized Mittag–Leffler function. This additional flexibility enables the description of crossover and complex relaxation behaviors beyond simple power-law memory, as illustrated schematically in Fig. 1. While this generalized operator provides enhanced flexibility for modeling complex systems, it is not always universally suitable for the entire available parameter regime, particularly for stochastic processes describing diffusion in heterogeneous or disordered media. In such cases, the solution must conform to the essential properties of a PDF, namely, normalization and non-negativity over the relevant domain. In this work, we derive reliable conditions on the model parameters to ensure these properties. We also analyze the resulting anomalous diffusion behavior by examining the MSD for the distributed-order systems.

[1] We use the sign $\simeq$ to denote asymptotic scaling neglecting constant coefficients.

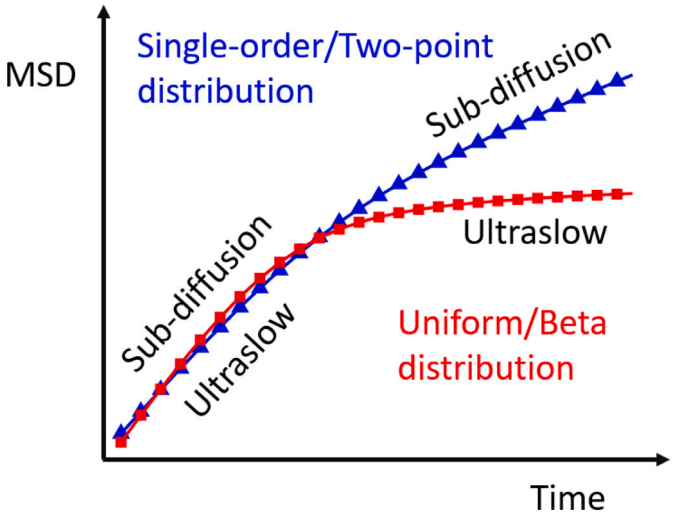

Fig. 1. Schematic illustration of the diffusion behaviors described by the HP-FDE for different distributed-order schemes considered in this paper: single-order, two-point, uniform, and Beta distributions. For the single-order and two-point distribution cases, the MSD exhibits crossover behavior between distinct subdiffusive regimes, whereas for the uniform and Beta distributions, transitions between different ultraslow diffusion regimes are observed.

The rest of this paper is structured as follows. In Section 2, we introduce and briefly review various definitions of fractional derivatives commonly employed in the modeling of complex systems. Section 3 presents the analysis of the single-order HP-FDE for both the force-free case and the case with a constant drift. In Section 4, we examine the solutions of the distributed-order HP-FDE and explore the anomalous diffusion behavior across three representative distributed-order scenarios. We summarize and discuss our results in Section 5.

2. Definitions of fractional derivatives

Before we consider the generalized HP-FDE, for the reader's convenience, in this section we provide a brief introduction to some definitions of fractional derivatives that are frequently employed in theoretical modeling and engineering. For more details, the reader can refer to Refs. [73,74].

2.1. Riemann–Liouville and Caputo derivatives

The RL-integral of order μ for a suitable function $f(t)$ is defined in terms of an integral with a power-law kernel [33,34]

$$I^{\mu}_{0^+} f(t) = \frac{1}{\Gamma(\mu)} \int_0^t \frac{f(t')}{(t-t')^{1-\mu}} dt' = \left(f * \Omega_{\mu}\right)(t), \tag{3}$$

with the kernel $\Omega_{\mu}(t) = t^{\mu-1}/\Gamma(\mu)$, and the operator $*$ denotes the standard convolution operator. The corresponding RL-derivative of the same order $\mu \in (0, 1]$ is defined as [33,34]

$$D^{\mu}_{0^+} f(t) = \frac{d}{dt} I^{1-\mu}_{0^+} f(t) = \frac{1}{\Gamma(1-\mu)} \frac{d}{dt} \int_0^t \frac{f(t')}{(t-t')^{\mu}} dt'. \tag{4}$$

The Caputo derivative of order $\mu \in (0, 1]$, for a suitable function $f(t)$ is defined [24,75,76]

$${}^{C}D^{\mu}_{0^+} f(t) = \frac{1}{\Gamma(1-\mu)} \int_0^t \frac{f'(t')}{(t-t')^{\mu}} dt', \tag{5}$$

where $f'(t) = df(t)/dt$.

Both the RL and Caputo fractional derivatives have (weak) singularities at $t = t'$. However, the Caputo derivative (5) is distinguished by containing the derivative of $f(t)$ inside the integral. This is in contrast to the RL fractional derivative (4), where differentiation occurs after fractional integration. In the Caputo formulation, when using Laplace transform methods to derive solutions, initial conditions enter in the traditional manner. For instance, for when $0 < \mu \leq 1$, the initial value of $f(t)$ at $t = 0$ is needed. In contrast, the RL-derivative leads to fractional-order initial conditions emerging.

2.2. Hilfer and Prabhakar derivatives

Hilfer derivatives [41–43], as a generalized fractional operator with the RL and the Caputo derivatives as specific cases is defined for order $\mu \in (0,1]$ and type parameter $\nu \in [0,1]$ by

$$D_{0+}^{\mu,\nu} f(t) = I_{0+}^{(1-\mu)\nu} \frac{d}{dt} \left(I_{0+}^{(1-\nu)(1-\mu)} f(t) \right). \tag{6}$$

Here definition (6) reduces to the RL-derivative (4) for $\nu = 0$ and to the Caputo derivative (5) for $\nu = 1$.

Another generalized fractional operator is the Prabhakar derivative [49], obtained through replacing the power-law kernel $\Omega_\mu(t) = t^{\mu-1}/\Gamma(\mu)$ in the RL integral (3) by the flexible memory kernel

$$e_{\rho,\mu}^{\gamma}(t) = t^{\mu-1} E_{\rho,\mu}^{\gamma}\left(-(\omega t)^{\rho}\right), \tag{7}$$

where the positive constant ω with physical unit $[\omega] = \text{time}^{-1}$ is introduced to get dimensions correct and

$$E_{\rho,\mu}^{\gamma}(z) = \sum_{k=0}^{\infty} \frac{\Gamma(\gamma+k)}{\Gamma(\gamma)\Gamma(\rho k+\mu)} \frac{z^k}{k!} \tag{8}$$

is the three-parameter generalized Mittag–Leffler function [48] characterized by three parameters $\rho, \mu > 0$, $\gamma \geq 0$. Alternatively, it can be also expanded for $|z| > 1$ as

$$E_{\rho,\mu}^{\gamma}(z) = \frac{(-z)^{\gamma}}{\Gamma(\gamma)} \sum_{k=0}^{\infty} \frac{\Gamma(\gamma+k)}{\Gamma(\mu-\rho(\gamma+k))} \frac{z^{-k}}{k!}. \tag{9}$$

The Laplace transform of the memory kernel (7) is given by [72,77,78]

$$\mathcal{L}\left[e_{\rho,\mu}^{\gamma}(t)\right] = \mathcal{L}\left[t^{\mu-1} E_{\rho,\mu}^{\gamma}\left(-(\omega t)^{\rho}\right)\right] = \frac{s^{\rho\gamma-\mu}}{(s^{\rho}+\omega^{\rho})^{\gamma}}. \tag{10}$$

The generalized Mittag–Leffler function exhibits the following asymptotic behavior [77]

$$E_{\rho,\mu}^{\gamma}(-(\omega t)^{\rho}) \sim \begin{cases} \dfrac{1}{\Gamma(\mu)}, & t \ll \omega^{-1} \\ \dfrac{(\omega t)^{-\rho\gamma}}{\Gamma(\mu-\rho\gamma)}, & t \gg \omega^{-1} \end{cases}. \tag{11}$$

Consequently, the kernel defined in Eq. (7) shows the asymptotic scaling

$$e_{\rho,\mu}^{\gamma}(t) \sim \begin{cases} \dfrac{t^{\mu-1}}{\Gamma(\mu)}, & t \ll \omega^{-1} \\ \dfrac{\omega^{-\rho\gamma} t^{\mu-\rho\gamma-1}}{\Gamma(\mu-\rho\gamma)}, & t \gg \omega^{-1} \end{cases}. \tag{12}$$

Fig. 2 depicts the memory kernel (7) in the Prabhakar integral, highlighting these distinct scalings for short and long times. It is important to note that the kernel (7) at short times ($t \ll \omega^{-1}$) is identical to that in the RL-integral (3). However, at long times ($t \gg \omega^{-1}$), when $\mu = \rho\gamma$, $e_{\rho,\mu}^{\gamma}(t)$ approaches a delta function $\delta(t)$ and when $\mu < \rho\gamma$, a negative relaxation mode is emerging: the kernel becomes negative and exhibits a power-law decay toward zero, as illustrated in the inset of Fig. 2. In fact, when the kernel changes sign, the operator effectively acts as a confined force on the right-hand side of the diffusion equation.

Applying the kernel (7) the Prabhakar integral is defined as [48,49]

$$\begin{aligned} \mathbf{E}_{\rho,\mu,0+}^{\gamma} f(t) &= \int_0^t (t-t')^{\mu-1} E_{\rho,\mu}^{\gamma}\left(-\omega^{\rho}(t-t')^{\rho}\right) f(t') dt' \\ &= \left(f * e_{\rho,\mu}^{\gamma}\right)(t). \end{aligned} \tag{13}$$

With the Prabhakar integral operator, the corresponding Prabhakar derivative of the order $\mu \in (0,1]$ is defined by differentiation after fractional integration,

$$D_{\rho,\mu,0+}^{\gamma} f(t) = \frac{d}{dt}\left(\mathbf{E}_{\rho,(1-\mu),0+}^{-\gamma} f(t)\right). \tag{14}$$

It is worth noting that the Prabhakar derivative (14) shares a structural similarity with the RL-derivative. Additionally, there exists a Caputo-type version of the Prabhakar derivative for order $\mu \in (0,1]$ defined as

$${}^{C}D_{\rho,\mu,0+}^{\gamma} f(t) = \mathbf{E}_{\rho,(1-\mu),0+}^{-\gamma} f'(t). \tag{15}$$

For $\gamma = 0$, the Prabhakar derivatives (14) and (15) reduce to the RL (4) and Caputo (5) fractional derivatives respectively.

We are now ready to define the Hilfer–Prabhakar (HP) derivative with order $\mu \in (0,1]$ and type parameter $\nu \in [0,1]$ combining the two forms of Prabhakar derivatives (14) and (15), given by [72,79]

$$D_{\rho,0+}^{\gamma,\mu,\nu} f(t) = \mathbf{E}_{\rho,\nu(1-\mu),0+}^{-\gamma\nu} \frac{d}{dt}\left(\mathbf{E}_{\rho,(1-\nu)(1-\mu),0+}^{-\gamma(1-\nu)} f(t)\right). \tag{16}$$

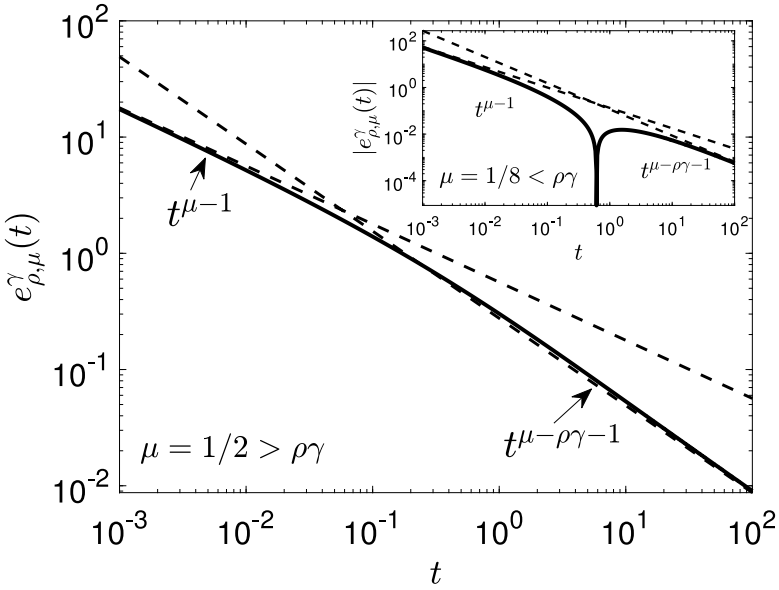

Fig. 2. Memory kernel (7) (solid curve) in the Prabhakar integral (13), with different asymptotic scalings (dashed lines) at short and long times given by (12). At short times, the behavior is identical to that of the RL-integral (3). Inset: when $\mu < \rho\gamma$, the kernel becomes negative at long times and approaches to zero in power-scaling form. Parameters: $\gamma = 1/2, \rho = 1/2, \omega = 1$.

The HP derivative simplifies to the Hilfer derivative (6) when $\gamma = 0$. Furthermore, when $\nu = 0$, the HP derivative reduces to the Prabhakar derivative of RL-type, given by (14), and when $\nu = 1$, it coincides with the Prabhakar derivative of Caputo-type, given by (15).

The Laplace transform of the HP derivative operator (16) with order $\mu \in (0, 1]$ and type $\nu \in [0, 1]$ is given by [72]

$$\mathcal{L}\left(D^{\gamma,\mu,\nu}_{\rho,0^+} f(t) \right)(s) = s^{\mu-\rho\gamma}(s^\rho + \omega^\rho)^\gamma \mathcal{L}(f)(s) - s^{-\nu(1-\mu+\rho\gamma)}(s^\rho + \omega^\rho)^{\gamma\nu} \times \mathbf{E}^{-\gamma(1-\nu)}_{\rho,(1-\nu)(1-\mu),0^+} f(t)\Big|_{t=0^+}, \tag{17}$$

which shows that the initial condition of the form

$$\mathbf{E}^{-\gamma(1-\nu)}_{\rho,(1-\nu)(1-\mu),0^+} f(t)\Big|_{t=0^+} \tag{18}$$

must be taken into account. However, such generalized initial conditions generally lack a clear physical interpretation unless either $\nu = 1$ or $\gamma = 0, \mu = 1$. As follows, we begin with FDEs involving the HP derivative with general initial conditions, and we demonstrate that the solution qualifies as a PDF only when integer-order initial conditions are recovered, i.e., when $\nu = 1$ or $\gamma = 0, \mu = 1$, the initial condition in Eq. (18) reduces to $f(0^+)$. In the first case ($\nu = 1$), the HP derivative reduces to the Caputo-type form (15), also referred to as the regularized version [72], which enables the modeling of anomalous diffusion in particle transport. In the second case ($\gamma = 0, \mu = 1$), it recovers the classical integer-order derivative leading to the diffusion equation for BM (normal diffusion).

3. Distributed-order HP-FDE: single-order

We begin with the FDE with HP derivative (16) and distributed-order of the weight function, for which we choose a PDF $p(\mu, \nu)$ of the order exponent and type parameter randomly chosen from $0 < \mu \leq 1$, and $0 \leq \nu \leq 1$ respectively and $p_M(\mu)$, $p_N(\nu)$ are the marginal distributions of $p(\mu, \nu)$,

$$p_M(\mu) = \int_0^\infty p(\mu, \nu) d\nu, \tag{19}$$

and

$$p_N(\nu) = \int_0^\infty p(\mu, \nu) d\mu. \tag{20}$$

The main equation is then given by

$$\int_0^1 \int_0^1 \tau^{\mu-1} p(\mu, \nu) D^{\gamma,\mu,\nu}_{\rho,0^+} W(x, t) d\mu d\nu = \mathscr{K} \frac{\partial^2}{\partial x^2} W(x, t), \tag{21}$$

where constant τ is introduced to get correct dimensions with physical unit $[\tau] = \text{time}$ and $\mathscr{K}$ is diffusion coefficient of physical unit $[\mathscr{K}] = \text{length}^2/\text{time}$. The solution $W(x, t)$ serves as the PDF for finding a particle at position x at time t. For the fractional orders

chosen in $(0,1]$, the solution function lies in the space of absolutely continuous functions on $[0,T]$, denoted as $AC([0,T])$. This space is equivalent to the Sobolev space $W^{1,1}[0,T]$.

The boundary condition is

$$\lim_{|x|\to\infty} W(x,t) = 0 \tag{22}$$

and the initial condition is[2]

$$\left[\mathbf{E}^{-\gamma(1-\nu)}_{\rho,(1-\nu)(1-\mu),0^+} W(x,t)\right]_{t=0^+} = \tau^{(1-\nu)(1-\mu)}\delta(x). \tag{23}$$

Especially for $\gamma = 0$ the HP derivative (16) reduces to the Hilfer derivative (6), and the above fractional initial condition becomes

$$\left[I^{(1-\mu)(1-\nu)}_{0^+} W(x,t)\right]_{t=0^+} = \tau^{(1-\nu)(1-\mu)}\delta(x). \tag{24}$$

Moreover, for $\nu = 0$, the fractional initial condition of the RL derivative is recovered, while for $\nu = 1$, it corresponds to the integer-order initial condition. Physically admissible initial conditions must correspond to local, finite, and directly interpretable probabilistic quantities, such as the initial probability density or its integer-order moments. This requirement is satisfied only in the Caputo-type case $\nu = 1$. In contrast, RL type initial conditions involve fractional derivatives evaluated at the initial time and implicitly depend on the prehistory of the process. As a result, they lead to fractional initial values that lack a clear probabilistic interpretation and, as demonstrated later, obstruct normalization of the probability density.

In this section, we consider the single-order HP-FDE of orders $\mu_0 \in (0,1]$ and type parameter $\nu_0 \in [0,1]$, which is a special case of the distributed-order FDE (21), such as

$$p(\mu,\nu) = \delta(\mu-\mu_0)\delta(\nu-\nu_0). \tag{25}$$

With these prerequisites, we obtain the FDE in the form

$$D^{\gamma,\mu_0,\nu_0}_{\rho,0^+} W(x,t) = K_{\mu_0}\frac{\partial^2}{\partial x^2} W(x,t). \tag{26}$$

where the generalized diffusion coefficient is $K_{\mu_0} = \mathscr{K}\tau^{1-\mu_0}$. Using a Laplace transform $\hat{W}(x,s) = \mathcal{L}[W(x,t)]$ given by (17) and a Fourier transform $\tilde{W}(k,t) = \mathcal{F}[W(x,t)]$, we obtain the solution in Fourier–Laplace domain

$$\tilde{\hat{W}}(k,s) = \frac{1}{s}\frac{(s\tau)^{1+\nu_0(\mu_0-\rho\gamma-1)}\left[(s\tau)^\rho+(\omega\tau)^\rho\right]^{\gamma\nu_0}}{(s\tau)^{\mu_0-\rho\gamma}\left[(s\tau)^\rho+(\omega\tau)^\rho\right]^{\gamma}+K_{\mu_0}\tau^{\mu_0}k^2}, \tag{27}$$

To investigate whether the solution $W(x,t)$ of the diffusion equation (26) qualifies as a PDF, we begin by verifying its normalization, i.e.,

$$\tilde{\hat{W}}(k=0,s) = \frac{\left[(s\tau)^\rho+(\omega\tau)^\rho\right]^{\gamma(\nu_0-1)}(s\tau)^{(\mu_0-\rho\gamma-1)(\nu_0-1)}}{s}. \tag{28}$$

In the time domain, the solution (28) corresponds to $\tilde{W}(k=0,t) = \int_{-\infty}^{\infty} W(x,t)dx$. If $W(x,t)$ is normalized, this quantity must equal unity for all t, i.e., $\tilde{W}(k=0,t) = 1$, which implies that its Laplace transform satisfies $\tilde{\hat{W}}(k=0,s) = 1/s$. Comparing this condition with Eq. (28), we conclude that $W(x,t)$ is normalized if and only if

$$\mu_0 = 1, \gamma = 0, \tag{29}$$

or

$$\nu_0 = 1. \tag{30}$$

When $\mu_0 = 1$ and $\gamma = 0$, the HP derivative (16) in the FDE (26) reduces to the classic integer-order derivative $dW(x,t)/dt$, and the solution (27) becomes

$$\tilde{\hat{W}}(k,s) = \frac{1}{s+K_1k^2}. \tag{31}$$

One can immediately arrive at the well-known Gaussian form PDF for the diffusion equation (1),

$$W(x,t) = \frac{1}{\sqrt{4\pi K_1 t}}\exp\left(-\frac{x^2}{4K_1t}\right). \tag{32}$$

For the second case when $\nu_0 = 1$, the solution (27) simplifies to

$$\tilde{\hat{W}}(k,s) = \frac{1}{s}\frac{R(s)}{R(s)+K_{\mu_0}k^2}, \tag{33}$$

[2] In the following, we show that the solution is a valid PDF when either $\nu = 1$ or $\mu = 1$; in both scenarios, the initial condition simplifies to the cases of integer-order.

where we define

$$R(s) = s^{\mu_0-\rho\gamma}(s^\rho + \omega^\rho)^\gamma. \tag{34}$$

Taking the inverse Fourier transform of (33) gives

$$\hat{W}(x,s) = \frac{1}{2s}\sqrt{\frac{R(s)}{K_{\mu_0}}}\exp\left(-\sqrt{\frac{R(s)}{K_{\mu_0}}}|x|\right). \tag{35}$$

Using Bernstein's theorem [80], which is briefly summarized in Appendix A, the non-negativity of the PDF $W(x,t)$ can be established by proving that its Laplace transform $\hat{W}(x,s)$ given in (35) is a completely monotone function (CMF). According to property (b) of the CMF in Appendix A, it is sufficient to prove that $\sqrt{R(s)}/(2s)$ and $\exp\left(-\sqrt{R(s)/K_{\mu_0}}|x|\right)$, are both CMFs. By applying properties (d), (f), and (g) of Bernstein functions (BFs) as listed in Appendix A, this reduces to demonstrate that $R(s)$ itself is a BF. According to the expression of $R(s)$ (34), under the conditions

$$0 \le \mu_0 - \rho\gamma \le 1, \quad 0 < \rho \le 1, \quad 0 \le \gamma \le 1, \tag{36}$$

it is sufficient to prove that $R(s)$ is a BF. To conclude, we emphasize that conditions (30) and (36) ensure that the single-order HP-FDE (26) admits a solution that qualifies as a valid PDF, thereby accurately describing anomalous diffusion of the particles in complex media. Later we will show that conditions (30) and (36) also hold for the single-order HP-FDE with drift, as well as for the distributed-order HP-FDE in Section 4.

We now examine the asymptotic behavior of the PDF (35). At short times $t \ll \omega^{-1}$, which corresponds to $s \gg \omega$ in the Laplace domain, then we approximate Eq. (34) as $R(s) \sim s^{\mu_0}$, and the solution (33) becomes

$$\tilde{\hat{W}}(k,s) \sim \frac{s^{\mu_0-1}}{s^{\mu_0} + K_{\mu_0}k^2}. \tag{37}$$

This leads to the following well-known solution of the FDE (26)

$$W(x,t) \sim \frac{1}{2\sqrt{K_{\mu_0}t^{\mu_0}}} M_{\mu_0/2}\left(\frac{|x|}{\sqrt{K_{\mu_0}t^{\mu_0}}}\right), \tag{38}$$

where M_z denotes the Mainardi function [81]. An alternative representation of the PDF is via Fox H-functions [11,82],

$$W(x,t) \sim \frac{1}{2|x|} H_{1,1}^{1,0}\left[\frac{|x|}{\sqrt{K_{\mu_0}t^{\mu_0}}}\,\middle|\,\begin{matrix}(1,\mu_0/2)\\(1,1)\end{matrix}\right] \sim \frac{1}{\sqrt{4\pi K_{\mu_0}t^{\mu_0}}} H_{2,0}^{1,2}\left[\frac{x^2}{4K_{\mu_0}t^{\mu_0}}\,\middle|\,\begin{matrix}(1-\mu_0/2,\mu_0)\\(0,1),(1/2,1)\end{matrix}\right]. \tag{39}$$

This solution at short times is identical to that in the FDE with Caputo or RL derivative [11].

And at long times $t \gg \omega^{-1}$, corresponding to $s \ll \omega$, then we have $R(s) \approx s^{\mu_0-\rho\gamma}$. Substituting back into Eq. (33), yields

$$\tilde{\hat{W}}(k,s) \sim \frac{\omega^{\rho\gamma}s^{\mu_0-\rho\gamma-1}}{\omega^{\rho\gamma}s^{\mu_0-\rho\gamma} + K_{\mu_0}k^2}, \tag{40}$$

and

$$W(x,t) \sim \frac{1}{\sqrt{4\pi K_{\mu_0}\omega^{-\rho\gamma}\ t^{\mu_0-\rho\gamma}}} H_{2,0}^{1,2}\left[\frac{x^2}{4K_{\mu_0}\omega^{-\rho\gamma}t^{\mu_0-\rho\gamma}}\,\middle|\,\begin{matrix}(1-(\mu_0-\rho\gamma)/2,\mu_0-\rho\gamma)\\(0,1),(1/2,1)\end{matrix}\right]. \tag{41}$$

The PDFs at short times (39) and at long times (41) have similar structure and using asymptotic expansion of the H function for large x [31,83], yields the stretched Gaussian behavior of the PDF [11]

$$W(x,t) \sim \frac{1}{\sqrt{4\pi K_{\mu_0}t^{\mu_0}}}\frac{1}{\sqrt{2-\mu_0}}\left(\frac{2}{\mu_0}\right)^{\frac{1-\mu_0}{2-\mu_0}}\left(\frac{|x|}{\sqrt{K_{\mu_0}t^{\mu_0}}}\right)^{-\frac{1-\mu_0}{2-\mu_0}} \times \exp\left(-\frac{2-\mu_0}{2}\left(\frac{\mu_0}{2}\right)^{\frac{\mu_0}{2-\mu_0}}\left(\frac{|x|}{\sqrt{K_{\mu_0}t^{\mu_0}}}\right)^{\frac{2}{2-\mu_0}}\right), \tag{42}$$

at short times and

$$\begin{aligned} W(x,t) \sim\ & \frac{1}{\sqrt{4\pi K_{\mu_0}\omega^{-\rho\gamma}t^{\mu_0-\rho\gamma}}}\frac{1}{\sqrt{2-\mu_0+\rho\gamma}} \\ & \times\left(\frac{2}{\mu_0-\rho\gamma}\right)^{\frac{1-\mu_0+\rho\gamma}{2-\mu_0+\rho\gamma}}\left(\frac{|x|}{\sqrt{K_{\mu_0}\omega^{-\rho\gamma}t^{\mu_0-\rho\gamma}}}\right)^{-\frac{1-\mu_0+\rho\gamma}{2-\mu_0+\rho\gamma}} \times \exp\left(-\frac{2-\mu_0+\rho\gamma}{2}\left(\frac{\mu_0-\rho\gamma}{2}\right)^{\frac{\mu_0-\rho\gamma}{2-\mu_0+\rho\gamma}}\left(\frac{|x|}{\sqrt{K_{\mu_0}\omega^{-\rho\gamma}t^{\mu_0-\rho\gamma}}}\right)^{\frac{2}{2-\mu_0+\rho\gamma}}\right) \end{aligned} \tag{43}$$

at long times. We note that, in both the short- and long-time limits, the PDFs can be expressed in terms of Fox H-functions given by Eqs. (39) and (41). The large-argument expansions of the Fox H-function are then used to derive stretched-Gaussian tails in

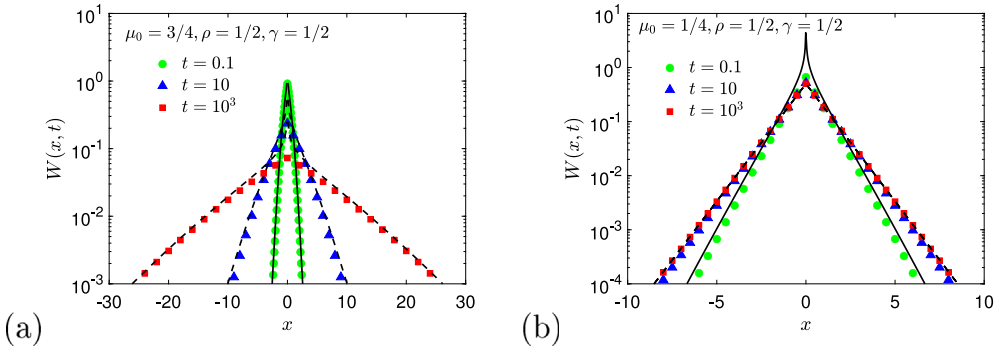

Fig. 3. Numerical solutions of the PDF of the HP-FDE (26) with (a) $\mu_0 = 3/4 > \rho\gamma$, (b) $\mu_0 = \rho\gamma = 1/4$. The numerical PDFs, represented by symbols (circles, triangles and squares), are obtained from the inverse Laplace transform of (35). The asymptotic PDFs (42) at short and (43) long times are represented by solid and dashed curves respectively. In particular, when $\mu_0 = \rho\gamma$, the PDF at long times is given by the Laplace distribution (44). Other Parameters: $\nu_0 = \omega = 1, K_{\mu_0} = 1/2$.

both regimes. Although the resulting asymptotic expressions in Eqs. (42) and (43) exhibit a similar stretched-Gaussian form, the corresponding exponents are different. This difference arises from the distinct asymptotic power-law scalings of the HP memory kernel defined in Eq. (7), as specified in Eq. (12). Consequently, the transport dynamics display different MSD behaviors in the short- and long-time limits, as demonstrated later in Eq. (48).

Fig. 3 illustrates the numerical PDFs of the single-order HP-FDE (26) in the force-free case, obtained from the inverse Laplace transform of (35). They have perfect agreement with the asymptotic stretched Gaussian form given by Eqs. (42) and (43). In particular, when $\mu_0 = \rho\gamma$, the solution (33) reduces to

$$\tilde{\tilde{W}}(k,s) \sim \frac{1}{s(1 + K_{\mu_0}\omega^{-\mu_0}k^2)}, \tag{44}$$

indicating the Laplace distribution

$$W(x,t) \sim \frac{1}{2\sqrt{K_{\mu_0}\omega^{-\mu_0}}} \exp\left(-\frac{|x|}{\sqrt{K_{\mu_0}\omega^{-\mu_0}}}\right), \tag{45}$$

which is stationary, i.e., independent of time, as shown in Fig. 3b.

The nth orders of moment can be derived by differentiating the solution (33) as follows

$$\langle x^n(t)\rangle = \mathcal{L}^{-1}\left[(i)^n \frac{\partial^n}{\partial k^n}\tilde{\tilde{W}}(k,s)\right]\Big|_{k=0} = \begin{cases} n!(K_{\mu_0})^{n/2}\mathcal{L}^{-1}\left[\dfrac{1}{s\,(R(s))^{n/2}}\right], & n \text{ is even} \\ 0, & n \text{ is odd} \end{cases}. \tag{46}$$

From this, the MSD follows

$$\langle x^2(t)\rangle = 2K_{\mu_0}t^{\mu_0}E^{\gamma}_{\rho,\mu_0+1}(-(\omega t)^{\rho}), \tag{47}$$

which exhibits the asymptotic behavior

$$\left\langle x^2(t)\right\rangle \sim \begin{cases} \dfrac{2K_{\mu_0}}{\Gamma(\mu_0+1)}t^{\mu_0}, & t \ll \omega^{-1} \\ \dfrac{2K_{\mu_0}\omega^{-\rho\gamma}}{\Gamma(\mu_0-\rho\gamma+1)}t^{\mu_0-\rho\gamma}, & t \gg \omega^{-1} \end{cases}. \tag{48}$$

As shown in Fig. 4, the short-time subdiffusive behavior t^{μ_0} is independent of the parameters ρ and γ, matching that of the classical FDEs with Caputo or RL derivatives, while for the long-time limit, the MSD changes to subdiffusion with scaling $t^{\mu_0-\rho\gamma}$. In particular, when $\mu_0 = \rho\gamma$, the MSD approaches a stationary value $\left\langle x^2(t)\right\rangle_{st} = 2K_{\mu_0}\omega^{-\mu_0}$. Moreover, for $\mu_0 < \rho\gamma$, the MSD decays as a power-law toward zero, however, this regime is excluded by the parameter constraints specified in (36). We also note that in this forbidden regime $\mu_0 < \rho\gamma$, the memory kernel (12) has a negative relaxation mode. Therefore, in the permitted parameter range the generalized HP-FDE is well-suited for modeling hybrid subdiffusive processes in complex environments, going beyond the capabilities of the traditional Caputo derivative.

3.1. Relation to the classic continuous time random walk

Here we discuss the relation of our HP-FDE (26) to the classic CTRW. First of all, we review the fundamental results of the CTRW and derive the corresponding diffusion equation in the case of the distributions of jumps $\lambda(x)$ and waiting times $\psi(t)$. The

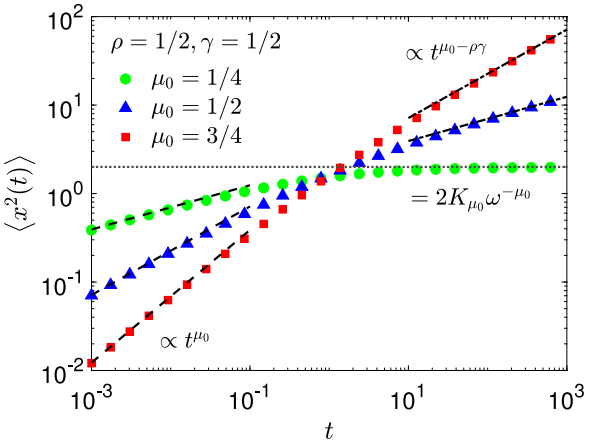

Fig. 4. Numerical solutions of the MSD of the single-order HP-FDE (26) from inverse Laplace transform of (46) are shown by colored symbols (circles, triangles and squares) for different μ_0 and fixed $\rho = 1/2, \gamma = 1/2$. The theoretical short- and long-time MSD scalings (48) are indicated by dashed and dot-dashed lines, respectively. The stationary MSD value for $\mu_0 = \rho\gamma$ is depicted with dotted lines. Other Parameters: $\nu_0 = \omega = 1, K_{\mu_0} = 1/2$.

PDF $W(x,t)$ of the displacement x and time t in the Fourier–Laplace space is given by the Montroll–Weiss equation [11,84,85]

$$\tilde{\hat{W}}(k,s) = \frac{1-\hat{\psi}(s)}{s}\frac{1}{1-\hat{\psi}(s)\tilde{\lambda}(k)}, \tag{49}$$

where $\tilde{\lambda}(k)$ is the Fourier transform of $\lambda(x)$. For any jump length PDF with finite variance, the limiting form of $\tilde{\lambda}(k)$ with $k \to 0$ is given by

$$\tilde{\lambda}(k) \sim 1 - k^2. \tag{50}$$

In Laplace space, the generalized waiting time PDF can be written in the simple form [86]

$$\hat{\psi}(s) = \frac{1}{1+s\hat{\theta}(s)}, \tag{51}$$

where $\theta(t)$ is a memory kernel. Rewriting Eq. (49) yields this limit

$$\hat{\theta}(s)\left[s\tilde{\hat{W}}(k,s) - 1\right] = -k^2\tilde{\hat{W}}(k,s). \tag{52}$$

After the inverse Fourier–Laplace transform, we obtain the FDE of the CTRW

$$\int_0^t \theta(t-t')\frac{\partial}{\partial t'}W(x,t')dt' = \frac{\partial^2}{\partial x^2}W(x,t), \tag{53}$$

with the memory kernel $\theta(t)$. The initial condition is of form $W(x,0) = \delta(x)$.

For the Caputo derivative with order μ_0, the corresponding kernel in the FDE have the form $\theta_C(t) = t^{-\mu_0}/\Gamma(1-\mu_0)$ and the waiting time PDF in the Laplace space $\hat{\psi}_C(s) = 1/(s^{\mu_0}+1)$ and in the time space $\psi_C(t) = t^{\mu_0-1}E_{\mu_0,\mu_0}\left(-t_0^{\mu}\right)$ [35]. In particular the waiting time PDF has a power-law tail, $\psi_C(t) \simeq t^{-(1+\mu_0)}$.

We rewrite our HP-FDE (26) with $\nu_0 = 1$ in the form

$$\int_0^t (t-t')^{-\mu_0}E^{-\gamma}_{\rho,1-\mu_0}\left(-\omega^\rho(t-t')^\rho\right)\frac{\partial}{\partial t'}W(x,t')dt' = K_{\mu_0}\frac{\partial^2}{\partial x^2}W(x,t), \tag{54}$$

and find that for the HP derivative, the corresponding kernel is

$$\theta(t) = t^{-\mu_0}E^{-\gamma}_{\rho,1-\mu_0}\left(-(\omega t)^\rho\right), \tag{55}$$

which exhibits the asymptotic behavior

$$\theta(t) \sim \begin{cases} \dfrac{1}{\Gamma(1-\mu_0)}t^{-\mu_0}, & t \ll \omega^{-1} \\ \dfrac{\omega^{\rho\gamma}}{\Gamma(1-\mu_0+\rho\gamma)}t^{-(\mu_0-\rho\gamma)}, & t \gg \omega^{-1} \end{cases}. \tag{56}$$

We note that when $\mu_0 = \rho\gamma$, $\theta(t) \sim 1$, leading to the diffusion equation of a steady-state solution (no time evolution).

Next we turn to waiting time PDF $\psi(t)$ of the HP-FDE in the Laplace space

$$\hat{\psi}(s) = \frac{1}{1+s\hat{\theta}(s)} = \frac{1}{1+s^{\mu_0-\rho\gamma}(\omega^\rho+s^\rho)^\gamma}. \tag{57}$$

We obtain the waiting time PDF for long times,

$$\lim_{t\to\infty}\psi(t)\sim\mathcal{L}^{-1}\left[\lim_{s\to 0}\hat{\psi}(s)\right]\sim\frac{\omega^{\rho\gamma}}{\Gamma(\mu_0-\rho\gamma)}t^{-(1+\mu_0-\rho\gamma)}. \tag{58}$$

Apart from the heavy tail, at short times, the waiting time PDF scales as

$$\lim_{t\to 0}\psi(t)\sim\mathcal{L}^{-1}\left[\lim_{s\to\infty}\hat{\psi}(s)\right]\sim\frac{1}{\Gamma(\mu_0)}t^{-(1+\mu_0)}. \tag{59}$$

This suggests that the HP-FDE can be derived as a continuum limit of a CTRW with a waiting time PDF with composite power-law scaling. At short times, the waiting times of the CTRW are chosen from the PDF $\simeq t^{-(1+\mu_0)}$, leading to the subdiffusion dynamics $\left\langle x^2(t)\right\rangle\simeq t^{\mu_0}$, and at long times, the waiting time PDF of the CTRW scales as $\simeq t^{-(1+\mu_0-\rho\gamma)}$, and the MSD changes to the modified subdiffusive scaling $\left\langle x^2(t)\right\rangle\simeq t^{\mu_0-\rho\gamma}$. We note in the CTRW picture, if $\mu_0\le\rho\gamma$, the waiting time PDF (57) is not normalized because $\hat{\psi}(0)\neq 1$. This implies that the HP-FDE can be related to CTRW only when $\mu_0>\rho\gamma$.

3.2. HP-FDE with drift

We consider single-order HP-FDE with a drift V_{μ_0} of physical dimension $[V_{\mu_0}]=\text{length/time}^{\mu_0}$,

$$D^{\gamma,\mu_0,\nu_0}_{\rho,0^+}W(x,t)=K_{\mu_0}\frac{\partial^2}{\partial x^2}W(x,t)-V_{\mu_0}\frac{\partial}{\partial x}W(x,t). \tag{60}$$

Similarly, using the Laplace and Fourier transformations for the diffusion equation with initial condition (23) and boundary condition (22), we obtain

$$\tilde{\hat{W}}(k,s)=\frac{1}{s}\frac{(s\tau)^{1+\nu_0(\mu_0-\rho\gamma-1)}\left[(s\tau)^\rho+(\omega\tau)^\rho\right]^{\gamma\nu_0}}{\left((s\tau)^{\mu_0-\rho\gamma}\left[(s\tau)^\rho+(\omega\tau)^\rho\right]^\gamma+\frac{\tau^{\mu_0}V_{\mu_0}^2}{4K_{\mu_0}}\right)+K_{\mu_0}\tau^{\mu_0}\left(k+\frac{V_{\mu_0}}{2K_{\mu_0}}i\right)^2}. \tag{61}$$

Obviously, when $\nu_0=1$, the solution is normalized because $\tilde{\hat{W}}(k=0,s)=1/s$. Accordingly, we will restrict our analysis to $\nu_0=1$ (for the other case $\gamma=0,\mu_0=1$, an integer-order derivative is recovered). Employing an inverse Fourier transformation yields the solution in Laplace domain,

$$\hat{W}(x,s)=\frac{\left(s^{-1}R(s)\right)}{\sqrt{4K_{\mu_0}R(s)+V_{\mu_0}^2}}\exp\left(\frac{V_{\mu_0}}{2K_{\mu_0}}x-\sqrt{\frac{R(s)}{K_{\mu_0}}+\frac{V_{\mu_0}^2}{4K_{\mu_0}^2}}|x|\right). \tag{62}$$

where $R(s)$ is given by Eq. (34). According to the conditions of the parameter (36), we have shown that $R(s)$ is a BF and thus $R(s)/s$ and $\sqrt{R(s)+V_{\mu_0}^2}/(4K_{\mu_0})$ are CMFs according to the properties (d) and (f) in Appendix A. To prove that the non-negativity of the solution, we just need to show that the exponential function in Eq. (62) is also a CMF, i.e.,

$$f(R(s))=\sqrt{\frac{R(s)}{K_{\mu_0}}+\frac{V_{\mu_0}^2}{4K_{\mu_0}^2}}\pm\frac{V_{\mu_0}}{2K_{\mu_0}} \tag{63}$$

is a BF, which can be easily shown with the fact that $f(s)$ is a BF since $f(s)\ge 0$ for all $s\ge 0$ and its derivative is a CMF.

Based on formula (46) we obtain the first moment

$$\langle x(t)\rangle=\mathcal{L}^{-1}\left[\frac{V_{\mu_0}}{sR(s)}\right]=V_{\mu_0}\mathcal{L}^{-1}\left[\frac{s^{\rho\gamma-\mu_0-1}}{(s^\rho+\omega^\rho)^\gamma}\right]=V_{\mu_0}t^{\mu_0}E^\gamma_{\rho,\mu_0^+1}(-(\omega t)^\rho), \tag{64}$$

and the second moment

$$\langle x^2(t)\rangle=\mathcal{L}^{-1}\left[\frac{2V_{\mu_0}^2}{sR^2(s)}+\frac{2K_{\mu_0}}{sR(s)}\right]=2V_{\mu_0}^2t^{2\mu_0}E^{2\gamma}_{\rho,2\mu_0^+1}(-(\omega t)^\rho)+2K_{\mu_0}t^{\mu_0}E^\gamma_{\rho,\mu_0^+1}(-(\omega t)^\rho). \tag{65}$$

Therefore we have the MSD

$$\begin{aligned}\left\langle\Delta x^2(t)\right\rangle&=\left\langle[x(t)-\langle x(t)\rangle]^2\right\rangle\\&=V_{\mu_0}^2t^{2\mu_0}\left[2E^{2\gamma}_{\rho,2\mu_0^+1}(-(\omega t)^\rho)-\left(E^\gamma_{\rho,\mu_0^+1}(-(\omega t)^\rho)\right)^2\right]+2K_{\mu_0}t^{\mu_0}E^\gamma_{\rho,\mu_0^+1}(-(\omega t)^\rho).\end{aligned} \tag{66}$$

At short times, the MSD exhibits

$$\left\langle\Delta x^2(t)\right\rangle\sim\left(\frac{2}{\Gamma(1+2\mu_0)}-\frac{1}{\Gamma(1+\mu_0)^2}\right)V_{\mu_0}^2t^{2\mu_0}+\frac{2K_{\mu_0}}{\Gamma(1+\mu_0)}t^{\mu_0}. \tag{67}$$

This suggests that in the short time limit, the subdiffusive scaling t^{μ_0} will dominate, as shown in Fig. 5 for different μ_0, corresponding to that of the Caputo-FDE with constant drift [35]. We note that when $\mu_0\neq 1$, the prefactor of the scaling $t^{2\mu_0}$ remains nonzero.

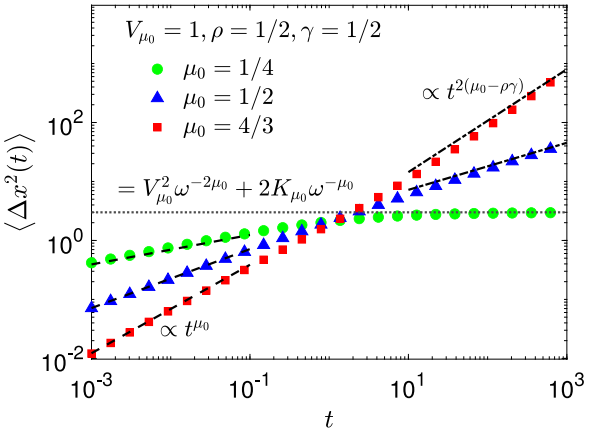

Fig. 5. Numerical MSDs of the single-order HP-FDE (60) with drift $V_{\mu_0} = 1$ from the inverse Laplace transform in (65) are shown by colored symbols (circles, triangles and squares) for different μ_0 and fixed $\rho = 1/2, \gamma = 1/2$. The theoretical short- and long-time MSD scalings (67) and (68) are indicated by dashed and dot-dashed lines, respectively. The stationary MSD value for $\mu_0 = \rho\gamma$ is depicted by dotted lines. Other Parameters: $\nu_0 = \omega = V_{\mu_0} = 1, K_{\mu_0} = 1/2$.

Whereas, at long times, the MSD changes to

$$\langle \Delta x^2(t) \rangle \sim \left(\frac{2}{\Gamma(1+2\mu_0-2\rho\gamma)} - \frac{1}{\Gamma(1+\mu_0-\rho\gamma)^2} \right) V_{\mu_0}^2 \omega^{-2\rho\gamma} t^{2(\mu_0-\rho\gamma)} + \frac{2K_{\mu_0}\omega^{-\rho\gamma}}{\Gamma(1+\mu_0-\rho\gamma)} t^{\mu_0-\rho\gamma}, \tag{68}$$

in which the drift term does not cancel when $\mu_0 - \rho\gamma \neq 1$ and will asymptotically dominate as shown in Fig. 5. Especially, when $\mu_0 - \rho\gamma > 1/2$, the MSD exhibits the superdiffusion and when $\mu_0 = \rho\gamma$, the MSD reduces the stationary value $V_{\mu_0}^2\omega^{-2\mu_0} + 2K_{\mu_0}\omega^{-\mu_0}$. We also observe that the ratio $\sqrt{\langle \Delta x^2(t) \rangle}/\langle x(t) \rangle$ at long times converges to a constant, which is similar to the observation in the subdiffusive CTRW. This property contrasts that of normal diffusion–advection, for which the ratio of the standard deviation over the mean decays to zero.

4. Distributed-order HP-FDE: general distributed order

In this section, we consider the HP-FDEs with distributed-order of weight function (21), where the weight function $p(\mu, \nu)$ for the order parameter μ and type parameter ν of the HP derivative satisfies Eqs. (19) and (20). We first analyze the properties of the corresponding solutions and then examine the resulting anomalous diffusion behavior in three representative distributed-order scenarios.

In the Fourier–Laplace domain, the solution of the HP-FDE (21) is given by

$$\tilde{\tilde{W}}(k,s) = \frac{1}{s} \frac{\int_0^1 \int_0^1 (s\tau)^{1+\nu(\mu-\rho\gamma-1)} [(s\tau)^\rho + (\omega\tau)^\rho]^{\gamma\nu} p(\mu,\nu) d\mu d\nu}{\int_0^1 (s\tau)^{\mu-\rho\gamma} [(s\tau)^\rho + (\omega\tau)^\rho]^\gamma p_M(\mu) d\mu + \mathscr{K}\tau k^2}. \tag{69}$$

The normalization condition $\tilde{\tilde{W}}(k=0,s) = 1/s$ for the solution can be expressed as

$$\frac{\int_0^1 \int_0^1 (s\tau)^{1+\nu(\mu-\rho\gamma-1)} [(s\tau)^\rho + (\omega\tau)^\rho]^{\gamma\nu} p(\mu,\nu) d\mu d\nu}{\int_0^1 (s\tau)^{\mu-\rho\gamma} [(s\tau)^\rho + (\omega\tau)^\rho]^\gamma p_M(\mu) d\mu} = 1. \tag{70}$$

Rewriting this expression, we obtain

$$\int_0^1 \int_0^1 \left[(s\tau)^{(\mu-\rho\gamma-1)(\nu-1)} \left((s\tau)^\rho + (\omega\tau)^\rho \right)^{\gamma(\nu-1)} - 1 \right] \times \left[(s\tau)^\rho + (\omega\tau)^\rho \right]^\gamma (s\tau)^{\mu-\rho\gamma} p_\nu(\nu) p_M(\mu) d\nu d\mu = 0, \tag{71}$$

which must hold for arbitrary distributions $p_M(\mu)$ and $p_N(\nu)$, and for all $s \geq 0$. This implies the integrand itself must vanish, that is

$$(s\tau)^{(\mu-\rho\gamma-1)(\nu-1)} \left((s\tau)^\rho + (\omega\tau)^\rho \right)^{\gamma(\nu-1)} = 1. \tag{72}$$

Since $\rho > 0$, this condition can only be satisfied for all $s \geq 0$ if both exponents are zero. This leads to $\gamma = 0, \mu = 1$ or $\nu = 1$, consistent with what we obtained in the single-order HP-FDE.

In the first case $\mu = 1, \gamma = 0$, the HP derivative reduces to the classical integer-order derivative, while in the second case $\nu = 1$, the HP derivative simplifies to the Caputo-type (15).

Next, we need to assess the non-negativity of the solution (69). Similar to the function $R(s) = s^{\mu_0-\rho\gamma}(s^\rho+\omega^\rho)^\gamma$, defined in Eq. (34), which qualifies as a BF under the conditions specified in (36), the function $Q(s) = (s\tau)^{\mu-\rho\gamma}\left[(s\tau)^\rho + (\omega\tau)^\rho\right]^\gamma$ is also expected to be a BF under the same conditions (36). Consequently, any linear combination of $Q(s)$, such as

$$\phi(s) = \int_0^1 (s\tau)^{\mu-\rho\gamma}\left[(s\tau)^\rho + (\omega\tau)^\rho\right]^\gamma p_M(\mu)d\mu \tag{73}$$

is also a BF. This ensures the non-negativity of the solution (69). It is important to note that values of the order parameter $\mu \in (0, \rho\gamma)$ constitute a forbidden regime where $P_M(\mu) = 0$, as they would violate the non-negativity of the solution.

Therefore, combining the conditions of the parameters (36) and $\nu = 1$, the HP-FDP with distributed order described by (21) simplifies to

$$\int_{\rho\gamma}^1 \tau^{\mu-1} p_M(\mu) D^{\gamma,\mu,1}_{\rho,0^+} W(x,t)d\mu = \mathscr{K}\frac{\partial^2}{\partial x^2}W(x,t), \tag{74}$$

and the initial condition (23) corresponds to the standard initial condition

$$\left[\mathbf{E}^0_{\rho,0,0^+} W(x,t)\right]_{t=0^+} = W(x,t=0) = \delta(x). \tag{75}$$

The solution in the Fourier–Laplace domain then has the form

$$\tilde{\tilde{W}}(k,s) = \frac{1}{s}\frac{\phi(s)}{\phi(s)+\mathscr{K}\tau k^2}, \tag{76}$$

where $\phi(s)$ is given by (73) and the corresponding MSD can be calculated as

$$\langle x^2(t)\rangle = \mathcal{L}^{-1}\left[-\frac{\partial^2}{\partial k^2}\tilde{\tilde{W}}(k,s)\right]\Bigg|_{k=0} = 2\mathscr{K}\tau\mathcal{L}^{-1}\left[\frac{1}{s\phi(s)}\right]. \tag{77}$$

Below, we present three representative cases for the distributed-order function $p_M(\mu)$: two-point distribution, uniform distribution, and beta distribution. For the two-point distribution, an analytical expression for the PDF can be obtained, while for the uniform and beta distributions, such exact solutions are not available. For each case, we analyze the resulting anomalous diffusion behavior governed by the corresponding FDEs.

4.1. Two-point distributed order

We first examine the case of the two-point distributed order defined by

$$p_M(\mu) = b_1\delta(\mu-\mu_1) + b_2\delta(\mu-\mu_2), \tag{78}$$

where the PDF is normalized as $b_1 + b_2 = 1$ and the range of μ_1 and μ_2 are in accordance with the admissible range defined by condition (36) and $\rho\gamma \le \mu_{1,2} \le 1$. Without loss of generality, we assume here $\mu_2 > \mu_1$.

In this scenario, the solution in the Fourier–Laplace domain takes the form

$$\tilde{\tilde{W}}(k,s) = \frac{1}{s}\frac{\phi(s)}{\phi(s)+\mathscr{K}\tau k^2}, \tag{79}$$

where

$$\phi(s) = \left[b_1(s\tau)^{\mu_1-\rho\gamma} + b_2(s\tau)^{\mu_2-\rho\gamma}\right]\left[(s\tau)^\rho + (\omega\tau)^\rho\right]^\gamma. \tag{80}$$

While this solution cannot be explicitly solved, for short times $t \ll \omega^{-1}$, that is $s \gg \omega$, we approximate

$$\phi(s) \sim b_1(s\tau)^{\mu_1} + b_2(s\tau)^{\mu_2}, \tag{81}$$

consequently,

$$\tilde{\tilde{W}}(k,s) \sim \frac{1}{s}\frac{b_1(s\tau)^{\mu_1} + b_2(s\tau)^{\mu_2}}{b_1(s\tau)^{\mu_1} + b_2(s\tau)^{\mu_2} + \mathscr{K}\tau k^2}. \tag{82}$$

By employing the series representation method described in [87] and performing an inverse Laplace transform, the solution can be expressed in terms of the three-parameter Mittag–Leffler function as

$$\begin{aligned} W(k,t) \sim \sum_{n=0}^{\infty}(-1)^n\left(\frac{b_1}{b_2}\right)^n\left(\frac{t}{\tau}\right)^{(\mu_2-\mu_1)n}\Bigg\{ & E^{n+1}_{\mu_2,(\mu_2-\mu_1)n+1}\left(-\frac{\mathscr{K}\tau k^2}{b_2}\left(\frac{t}{\tau}\right)^{\mu_2}\right) \\ & + \frac{b_1}{b_2}\left(\frac{t}{\tau}\right)^{\mu_2-\mu_1} E^{n+1}_{\mu_2,(\mu_2-\mu_1)(n+1)+1}\left(-\frac{\mathscr{K}\tau k^2}{b_2}\left(\frac{t}{\tau}\right)^{\mu_2}\right)\Bigg\}. \end{aligned} \tag{83}$$

To obtain the inverse Fourier transform of the above solution, we utilize the relationship between the three-parameter Mittag–Leffler function, the H-function, and the Mellin cosine transform, used in [77]. The PDF is given by

$$W(x,t) = \frac{1}{\sqrt{4\pi[\mathscr{K}\tau/b_2](t/\tau)^{\mu_2}}}\sum_{n=0}^{\infty}(-1)^n\left(\frac{b_1}{b_2}\right)^n\left(\frac{t}{\tau}\right)^{(\mu_2-\mu_1)n}$$

$$\times \left\{ H_{1,2}^{2,0}\left[\frac{x^2}{4[\mathscr{K}\tau/b_2](t/\tau)^{\mu_2}} \middle| \begin{matrix} ((\mu_2-\mu_1)n+1-\mu_2/2,\mu_2) \\ (0,1),(n+1/2,1) \end{matrix} \right] + \frac{\mu_1}{\mu_2}\left(\frac{t}{\tau}\right)^{\mu_2-\mu_1} \right.$$
$$\left. \times H_{1,2}^{2,0}\left[\frac{x^2}{4[\mathscr{K}\tau/b_2](t/\tau)^{\mu_2}} \middle| \begin{matrix} ((\mu_2-\mu_1)(n+1)+1-\mu_2/2,\mu_2) \\ (0,1),(n+1/2,1) \end{matrix} \right] \right\}. \tag{84}$$

A similar analysis carried out for long times $t \gg \omega^{-1}$, (i.e., $s \ll \omega$) yields

$$\phi(s) \sim (\omega\tau)^{\rho\gamma}\left[b_1(s\tau)^{\mu_1-\rho\gamma} + b_2(s\tau)^{\mu_2-\rho\gamma}\right], \tag{85}$$

such that

$$\tilde{\tilde{W}}(k,s) \sim \frac{1}{s}\frac{(\omega\tau)^{\rho\gamma}\left[b_1(s\tau)^{\mu_1-\rho\gamma} + b_2(s\tau)^{\mu_2-\rho\gamma}\right]}{(\omega\tau)^{\rho\gamma}\left[b_1(s\tau)^{\mu_1-\rho\gamma} + b_2(s\tau)^{\mu_2-\rho\gamma}\right] + \mathscr{K}\tau k^2}. \tag{86}$$

By following the same procedure, the PDF at long times can be obtained by substituting the exponents $\mu_1 \to \mu_1 - \rho\gamma$, $\mu_2 \to \mu_2 - \rho\gamma$ and $\mathscr{K} \to \mathscr{K}/(\omega\tau)^{\rho\gamma}$ into the short-time PDF in Eq. (84).

The MSD can be derived using Eq. (77), and its asymptotic behavior is analyzed below. Combining Eqs. (81) and (85) we obtain

$$\left\langle x^2(t)\right\rangle \sim \begin{cases} \frac{2\mathscr{K}\tau}{b_2}\left(\frac{t}{\tau}\right)^{\mu_2} E_{\mu_2-\mu_1,\mu_2+1}\left(-\frac{b_1}{b_2}\left(\frac{t}{\tau}\right)^{\mu_2-\mu_1}\right), & t \ll \omega^{-1} \\ \frac{2\mathscr{K}\tau}{b_2(\omega\tau)^{\rho\gamma}}\left(\frac{t}{\tau}\right)^{\mu_2-\rho\gamma} E_{\mu_2-\mu_1,\mu_2+1-\rho\gamma}\left(-\frac{b_1}{b_2}\left(\frac{t}{\tau}\right)^{\mu_2-\mu_1}\right), & t \gg \omega^{-1} \end{cases}. \tag{87}$$

Furthermore, when $\mu_2 > \mu_1$, by applying the asymptotic approximation of the generalized Mittag–Leffler function given in (11), the MSD asymptotically scales as

$$\left\langle x^2(t)\right\rangle \sim \begin{cases} \frac{2\mathscr{K}\tau}{b_2\Gamma(1+\mu_2)}\left(\frac{t}{\tau}\right)^{\mu_2}, & t \ll \{\omega^{-1},\tau\} \\ \frac{2\mathscr{K}\tau}{b_2(\omega\tau)^{\rho\gamma}\Gamma(1+\mu_1-\rho\gamma)}\left(\frac{t}{\tau}\right)^{\mu_1-\rho\gamma}, & t \gg \{\omega^{-1},\tau\} \end{cases}. \tag{88}$$

The asymptotic behavior of the MSD is shown in Fig. 6a, in perfect agreement with the numerical results obtained from the inverse Laplace transform (77). This indicates that when multiple characteristic scales are embedded in the order distribution $P_M(\mu)$ in Eq. (78) with $\mu_2 > \mu_1$, the larger exponent μ_2 governs the short-time dynamics, whereas the smaller exponent μ_1 emerges in the long-time regime.

4.2. Uniform distributed order

We next consider a uniform distributed order with

$$p_M(\mu) = \frac{1}{1-\rho\gamma} \tag{89}$$

which is normalized in the range $\rho\gamma \le \mu \le 1$. Substituting this distribution into Eq. (73), we obtain

$$\phi(s) = \frac{\left[(s\tau)^{1-\rho\gamma} - 1\right]\left[(s\tau)^{\rho} + (\omega\tau)^{\rho}\right]^{\gamma}}{(1-\rho\gamma)\log(s\tau)}. \tag{90}$$

The corresponding asymptotic behavior is then given by

$$\phi(s) \sim \begin{cases} \frac{1}{1-\rho\gamma}\frac{s\tau}{\log(s\tau)}, & s \gg \{\omega,\tau^{-1}\} \\ \frac{(\omega\tau)^{\rho\gamma}}{1-\rho\gamma}\frac{1}{\log(1/(s\tau))}, & s \ll \{\omega,\tau^{-1}\} \end{cases}. \tag{91}$$

Using the MSD formula (46) along with the Tauberian theorem [80] (see also Appendix B), we find

$$\left\langle x^2(t)\right\rangle \sim \begin{cases} 2\mathscr{K}\tau(1-\rho\gamma)\left(\frac{t}{\tau}\right)\log\left(\frac{\tau}{t}\right), & t \ll \{\omega^{-1},\tau\} \\ 2\mathscr{K}\tau(1-\rho\gamma)\log\left(\frac{t}{\tau}\right), & t \gg \{\omega^{-1},\tau\} \end{cases}. \tag{92}$$

This result indicates that in the short time limit, the MSD approach zero while in the long time limit MSD exhibits ultraslow diffusion with logarithmic growth. The numerical MSD and the theoretical results for the HP-FDE with uniform distribution are shown in Fig. 6b.

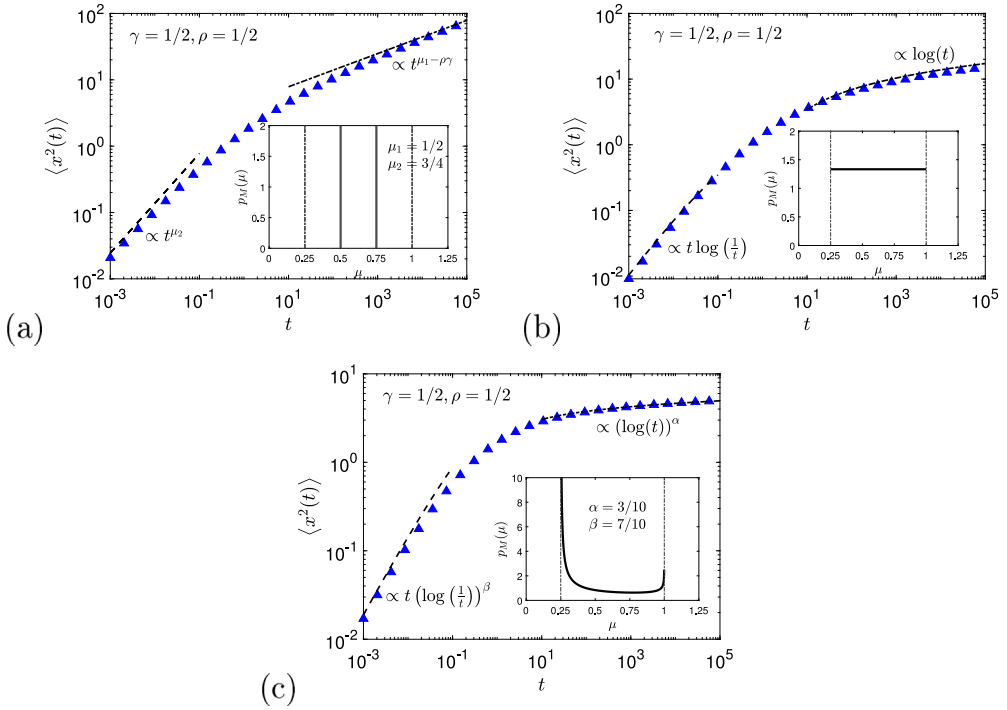

Fig. 6. MSDs for the distributed-order HP-FDE with (a) two-point distribution (78) $\mu_1 = 1/2, \mu_2 = 3/4$, (b) uniform distribution (89), (c) beta distribution (93) with $\alpha = 3/10, \beta = 7/10$. The numerical results for the MSD from (77) are represented by blue triangles. The asymptotic MSDs at short and long times given by (88), (92) and (100) are represented by dashed and dot-dashed lines respectively. Inset: the distribution of the order $P_M(\mu)$, the general admissible regime of the order $\rho\gamma \le \mu \le 1$ is represented by dot-dashed lines. Other Parameters: $P_N(\nu) = \delta(\nu - 1), \omega = \tau = 1, \mathscr{K} = 1/2$.

4.3. Beta distributed order

Next, we consider the beta-distributed order case defined by

$$p_M(\mu) = \frac{(\mu - \rho\gamma)^{\alpha-1}(1-\mu)^{\beta-1}}{B(\alpha,\beta)(1-\rho\gamma)^{\alpha+\beta-1}}, \tag{93}$$

which is normalized in the range $\rho\gamma \le \mu \le 1$,. Here $\alpha, \beta > 0$ are shape parameters and $B(\alpha,\beta) = \Gamma(\alpha)\Gamma(\beta)/\Gamma(\alpha+\beta)$ is the Beta function [88].

In this case, the function $\phi(s)$ (73) can be expressed as

$$\begin{aligned}\phi(s) &= \frac{\left[(s\tau)^{\rho} + (\omega\tau)^{\rho}\right]^{\gamma}}{B(\alpha,\beta)(1-\rho\gamma)^{\alpha+\beta-1}} \int_{\rho\gamma}^{1} (\mu-\rho\gamma)^{\alpha-1}(1-\mu)^{\beta-1}(s\tau)^{\mu-\rho\gamma}\, d\mu \\ &= \left[(s\tau)^{\rho} + (\omega\tau)^{\rho}\right]^{\gamma} {}_1F_1(\alpha, \alpha+\beta, (1-\rho\gamma)\log(s\tau)).\end{aligned} \tag{94}$$

Here ${}_1F_1(a,b,z)$ is a confluent hypergeometric function (Kummer function) [88]

$${}_1F_1(a,b,z) = \frac{\Gamma(b)}{\Gamma(b-a)\Gamma(a)} \int_0^1 e^{zt} t^{a-1}(1-t)^{b-a-1}\, \mathrm{d}t. \tag{95}$$

At short times $t \ll \{\omega^{-1}, \tau\}$,i.e., $s \gg \{\omega, \tau^{-1}\}$, using the asymptotic form of the confluent hypergeometric function for large z [88],

$${}_1F_1(a,b,z) \sim \Gamma(b)/\Gamma(a) e^z z^{a-b}, \tag{96}$$

we find

$$\phi(s) \sim \frac{\Gamma(\alpha+\beta)}{\Gamma(\alpha)(1-\rho\gamma)^{\beta}} \frac{s\tau}{[\log(s\tau)]^{\beta}}. \tag{97}$$

At long times $t \gg \{\omega^{-1}, \tau\}$, i.e., $s \ll \{\omega, \tau^{-1}\}$, using the property

$${}_1F_1(a,b,z) = e^z {}_1F_1(b-a, b, -z) \tag{98}$$

Table 1
Comparison of the HP-FDE for various distributed-order schemes, including single-order, two-point, uniform, and Beta distributions, summarizing the admissible general parameter regimes, the specified parameters for each distribution, and the associated MSD scaling behaviors.

Distribution $P_M(\mu)$	General parameters	Specified parameters	MSD
$\delta(\mu-\mu_0)$		$\rho\gamma \le \mu_0 \le 1$	ST: $\sim \frac{2K_{\mu_0}}{\Gamma(\mu_0+1)} t^{\mu_0}$, (48)
			LT: $\sim \frac{2K_{\mu_0}\omega^{-\rho\gamma}}{\Gamma(\mu_0-\rho\gamma+1)} t^{\mu_0-\rho\gamma}$ (48)
$b_1\delta(\mu-\mu_1)$ $+b_2\delta(\mu-\mu_2)$	$\nu=1$ $\rho\in(0,1]$ $\gamma\in[0,1]$	$\rho\gamma \le \mu_1 < \mu_2 \le 1$ $b_1+b_2=1$	ST: $\sim \frac{2\mathscr{K}\tau}{b_2\Gamma(1+\mu_2)}\left(\frac{t}{\tau}\right)^{\mu_2}$, (88)
			LT: $\sim \frac{2\mathscr{K}\tau}{b_2(\omega\tau)^{\rho\gamma}\Gamma(1+\mu_1-\rho\gamma)}\left(\frac{t}{\tau}\right)^{\mu_1-\rho\gamma}$ (88)
$\frac{1}{1-\rho\gamma}$		/	ST: $\sim 2\mathscr{K}\tau(1-\rho\gamma)\left(\frac{t}{\tau}\right)\log\left(\frac{\tau}{t}\right)$, (92)
			LT: $\sim 2\mathscr{K}\tau(1-\rho\gamma)\log\left(\frac{t}{\tau}\right)$ (92)
$\frac{(\mu-\rho\gamma)^{\alpha-1}(1-\mu)^{\beta-1}}{B(\alpha,\beta)(1-\rho\gamma)^{\alpha+\beta-1}}$		$\alpha,\beta>0$	ST: $\sim \frac{2\mathscr{K}\tau\Gamma(\alpha)(1-\rho\gamma)^{\beta}}{\Gamma(\alpha+\beta)}\left(\frac{t}{\tau}\right)\left[\log\left(\frac{\tau}{t}\right)\right]^{\beta}$, (100)
			LT: $\sim \frac{2\mathscr{K}\tau\Gamma(\beta)(1-\rho\gamma)^{\alpha}}{\Gamma(\alpha+\beta)(\omega\tau)^{\rho\gamma}}\left[\log\left(\frac{t}{\tau}\right)\right]^{\alpha}$, (100)

of the confluent hypergeometric function [88], we get

$$\phi(s) \sim \frac{\Gamma(\alpha+\beta)(\omega\tau)^{\rho\gamma}}{\Gamma(\beta)(1-\rho\gamma)^{\alpha}} \frac{1}{[\log(1/s)]^{\alpha}}. \tag{99}$$

By applying the Tauberian theorem [80], the MSD behaves asymptotically as

$$\left\langle x^2(t)\right\rangle \sim \begin{cases} \dfrac{2\mathscr{K}\tau\Gamma(\alpha)(1-\rho\gamma)^{\beta}}{\Gamma(\alpha+\beta)}\left(\dfrac{t}{\tau}\right)\left[\log\left(\dfrac{\tau}{t}\right)\right]^{\beta}, & t \ll \{\omega^{-1},\tau\} \\ \dfrac{2\mathscr{K}\tau\Gamma(\beta)(1-\rho\gamma)^{\alpha}}{\Gamma(\alpha+\beta)(\omega\tau)^{\rho\gamma}}\left[\log\left(\dfrac{t}{\tau}\right)\right]^{\alpha}, & t \gg \{\omega^{-1},\tau\} \end{cases}. \tag{100}$$

Thus, at short times the diffusion is linear in time, with a logarithmic correction, while the long time behavior is ultraslow, as shown in Fig. 6c.

5. Discussion and conclusions

In this paper, we propose the distributed-order HP-FDE, as a powerful modeling framework for capturing both composite subdiffusive and ultraslow diffusion behaviors of particles in complex media. We derive the exact solution in the Fourier–Laplace domain and identify a permissible range of parameters within which the solution satisfies the requirements of a valid PDF which should be normalized and non-negative, when the HP derivative reduces to the Caputo form under standard integer-order initial conditions. For the single-order case, we analyze the asymptotic behavior of the PDF at short and long times using the Fox H-function, with stretched Gaussian tails. These distinct PDFs at short and long times lead to the different subdiffusive dynamics. For the distributed-order FDE, we also obtain the general solution, and provide the asymptotic MSDs for three representative order distributions: two-point, uniform, and beta distributions. Notably, the uniform and beta cases exhibit ultraslow diffusion. The main results are summarized in Table 1.

While the HP derivative generalizes the classical Riemann–Liouville and Caputo derivatives by incorporating a three-parameter Mittag–Leffler kernel, thereby enabling more complex dynamical behaviors due to its increased parameter flexibility, its application to diffusion equations requires careful parameter constraints. This is particularly important when the solution is interpreted as a PDF describing stochastic particle transport in complex media. To ensure that the solution remains normalized, the HP derivative must reduce to the Caputo-type form. Furthermore, preserving the non-negativity of the solution necessitates that model parameters remain within an admissible range (36), excluding regimes that yield non-physical results—for example, when $\mu < \rho\gamma$, the MSD can decay to zero at long times in both single-order and distributed-order cases. We hope this work offers practical guidance for experimentalists aiming to use HP-FDE in modeling particle transport, by emphasizing the importance of maintaining physical consistency through appropriate parameter selection.

The FDE with a given order of the HP fractional time derivative are closely connected to the CTRW processes with the generalized distribution of waiting times exhibiting two distinct power-law tails, as indicated by Eqs. (58) and (59) . However, a direct correspondence between distributed-order FDEs and CTRWs has not yet been fully established. In [51], a comparison was drawn between distributed-order FDEs and more generalized CTRW models, incorporating random trapping times governed by a variable order β with an associated PDF $p(\beta)$. By introducing a conditional waiting time distribution $\psi(t|\beta)$, they formulated the overall waiting time PDF $\psi(t) = \int_0^1 p(\beta)\psi(t|\beta)d\beta$, where the order β ranges within $[0,1]$.

An ideal application of the HP-FDE is transport of particles in complex systems with heterogeneous environments or multiple trapping mechanisms [89–92], where such structural complexity naturally leads to crossover behaviors across distinct time scales.

The parameters appearing in the HP fractional derivative can be appropriately chosen to model concrete physical systems. For instance, in the case of an HP derivative with a single fractional order μ, the parameters μ and $\rho\gamma$ (with $\nu = 1$, which we show is required to ensure that the solution constitutes a proper PDF) can be inferred from the distinct scaling exponents of the transport dynamics at short and long times. In addition, advanced numerical approach should also developed to solve the FDE with distributed orders [93] involving the HP derivative, particularly in the presence of confined nonlinear external forces or reflecting/absorbing boundary conditions. Beyond the diffusion equation framework, the Langevin equation offers another powerful formalism for describing anomalous diffusion, particularly in single-particle tracking, a standard technique in biological experiments [12,53,94]. In future work, incorporating the HP derivative into the Langevin framework may provide new insights, and the resulting statistical properties of such models remain an open area of investigation. Similarly, time dependent or stochastic scaling exponents as studied in the context of fractional Brownian motion [95–101] will be of interest in the modeling of heterogeneous complex media.

CRediT authorship contribution statement

Wei Wang: Writing – review & editing, Visualization, Methodology, Investigation, Data curation, Conceptualization. **Ralf Metzler:** Writing – review & editing, Validation, Supervision, Methodology. **Živorad Tomovski:** Writing – review & editing, Writing – original draft, Validation, Supervision, Methodology, Investigation, Conceptualization.

Declaration of competing interest

The authors declare that they have no competing interests.

Acknowledgments

R.M. acknowledges financial support from the German Science Foundation (DFG grants ME 1535/22-1 and Project-ID 318763901 CRC1294 Data Assimilation, project B10), and NSF-BMBF CRCNS (Grant No. 2112862/STAXS). Z.T. acknowledges the support by the project 24-10177L, GACR (LA granty) "Fractional and fuzzy-fractional transport in disordered environments".

Appendix A. Completely monotone and Bernstein functions

Here we recall some definitions and properties of completely monotone functions (CMF) and Bernstein functions (BF) [102] which are used to show the non-negativity of the fundamental solution.

A.1. Completely monotone functions

A CMF $\mathcal{M}(s)$ is defined on the non-negative semi-axis and has the property

$$(-1)^n \mathcal{M}^{(n)}(s) \geq 0 \quad \text{for all } n \in \mathrm{N}_0 \text{ and } s \geq 0. \tag{A.1}$$

According to Bernstein theorem the CMF can be represented as a Laplace transform of a non-negative function $p(t)$ (see, for example, Chapter XIII, Section 4 in Ref. [80]), i.e.,

$$\mathcal{M}(s) = \int_0^\infty p(t) e^{-st}\, dt. \tag{A.2}$$

The following properties hold true for a CMF:

(**a**) A linear combination $a_1\mathcal{M}_1(s) + a_2\mathcal{M}_2(s)$ $(a_1, a_2 \geq 0)$ of CMFs $\mathcal{M}_1(s)$ and $\mathcal{M}_2(s)$ is a CMF as well.
(**b**) The product $\mathcal{M}(s) = \mathcal{M}_1(s)\mathcal{M}_2(s)$ of CMFs $\mathcal{M}_1(s)$ and $\mathcal{M}_2(s)$ is again a CMF.

An example of a CMF is s^α, where $\alpha \leq 0$.

A.2. Bernstein functions

A BF is a non-negative function whose derivative is a CMF, that is,

$$(-1)^{(n-1)} \mathcal{B}^{(n)}(s) \geq 0 \quad \text{for all } n \in \mathrm{N}_0 \text{ and } s \geq 0. \tag{A.3}$$

BFs have the following properties:

(**c**) A linear combination $a_1\mathcal{B}_1(s) + a_2\mathcal{B}_2(s)$ $(a_1, a_2 \geq 0)$ of BFs $\mathcal{B}_1(s)$ and $\mathcal{B}_2(s)$ is a BF.
(**d**) If $\mathcal{B}(s)$ is a BF, then $\mathcal{B}(s)/s$ is a CMF.
(**e**) A composition $\mathcal{M}(\mathcal{B}(s))$ of a CMF $\mathcal{M}(s)$ and a BF $\mathcal{B}(s)$ is a CMF.
(**f**) A composition $\mathcal{B}_1(\mathcal{B}_2(s))$ of BFs is again a BF.
(**g**) From these properties it follows that the function $e^{-u\,\mathcal{B}(s)}$ is a CMF for all $u > 0$ if $\mathcal{B}(s)$ is a BF.

An example of a BF is s^α, where $0 \leq \alpha \leq 1$.

Appendix B. Tauberian theorem [80]

Let $L(t)$ be a slowly varying function, i.e. $\lim_{t\to\infty} L(at)/L(t) = 1$, for all $a > 0$. If

$$\hat{R}(s) = \mathcal{L}[r(t)] \simeq s^{-\rho} L\left(\frac{1}{s}\right), \quad s \to 0, \quad \rho \geq 0, \tag{B.1}$$

then

$$r(t) = \mathcal{L}^{-1}[\hat{R}(s)] \simeq \frac{1}{\Gamma(\rho)} t^{\rho-1} L(t), \quad t \to \infty. \tag{B.2}$$

It also applies without change when the roles of infinity and zero are interchanged, that is, if

$$\hat{R}(s) = \mathcal{L}[r(t)] \simeq s^{-\rho} L(s), \quad s \to \infty, \quad \rho \geq 0, \tag{B.3}$$

then

$$r(t) = \mathcal{L}^{-1}[\hat{R}(s)] \simeq \frac{1}{\Gamma(\rho)} t^{\rho-1} L\left(\frac{1}{t}\right), \quad t \to 0. \tag{B.4}$$

Data availability

Data will be made available on request.

References

[1] R. Brown, A brief account of microscopical observations made in the months of June, July and August 1827, on the particles contained in the pollen of plants; and on the general existence of active molecules in organic and inorganic bodies, Phil. Mag. 4 (1828) 161.
[2] A. Einstein, Über die von der molekularkinetischen Theorie der Wärme geforderte Bewegung von in ruhenden Flüssigkeiten suspendierten Teilchen, Ann. Phys. 322 (1905) 549.
[3] M. Weiss, M. Elsner, F. Kartberg, T. Nilsson, Anomalous subdiffusion is a measure for cytoplasmic crowding in living cells, Biophys. J. 87 (2004) 3518.
[4] I. Golding, E.C. Cox, Physical nature of bacterial cytoplasm, Phys. Rev. Lett. 96 (2006) 098102.
[5] J.-H. Jeon, V. Tejedor, S. Burov, E. Barkai, C. Selhuber-Unkel, K. Berg-Sørensen, L. Oddershede, R. Metzler, In vivo anomalous diffusion and weak ergodicity breaking of lipid granules, Phys. Rev. Lett. 106 (2011) 048103.
[6] R. Großmann, L.S. Bort, T. Moldenhawer, M. Stange, S.S. Panah, R. Metzler, C. Beta, Non-Gaussian displacements in active transport on a carpet of motile cells, Phys. Rev. Lett. 132 (2024) 088301.
[7] J.-H. Jeon, M. Javanainen, H. Martinez-Seara, R. Metzler, I. Vattulainen, Protein crowding in lipid bilayers gives rise to non-Gaussian anomalous lateral diffusion of phospholipids and proteins, Phys. Rev. X 6 (2016) 021006.
[8] A. Godec, M. Bauer, R. Metzler, Collective dynamics effect transient subdiffusion of inert tracers in flexible gel networks, New J. Phys. 16 (2016) 092002.
[9] T. Akimoto, E. Yamamoto, K. Yasuoka, Y. Hirano, M. Yasui, Non-Gaussian fluctuations resulting from power-law trapping in a lipid bilayer, Phys. Rev. Lett. 107 (2011) 178103.
[10] R. Metzler, J. Klafter, The restaurant at the end of the random walk: recent developments in the description of anomalous transport by fractional dynamics, J. Phys. A: Math. Gen. 37 (2004) R161.
[11] R. Metzler, J. Klafter, The random walk's guide to anomalous diffusion: A fractional dynamics approach, Phys. Rep. 339 (2000) 1.
[12] R. Metzler, J.-H. Jeon, A.G. Cherstvy, E. Barkai, Anomalous diffusion models and their properties: Non-stationarity, non-ergodicity, and ageing at the centenary of single particle tracking, Phys. Chem. Chem. Phys. 16 (2014) 24128.
[13] E. Barkai, R. Metzler, J. Klafter, From continuous time random walks to the fractional Fokker–Planck equation, Phys. Rev. E 61 (2000) 132.
[14] A. Compte, Stochastic foundations of fractional dynamics, Phys. Rev. E 53 (1996) 4191.
[15] R. Hilfer, L. Anton, Fractional master equations and fractal time random walks, Phys. Rev. E 51 (1995) R848(R).
[16] R. Metzler, E. Barkai, J. Klafter, Anomalous diffusion and relaxation close to thermal equilibrium: A fractional Fokker–Planck equation approach, Phys. Rev. Lett. 82 (1999) 3563.
[17] E. Barkai, Fractional Fokker–Planck equation, solution, and application, Phys. Rev. E 63 (2001) 046118.
[18] F. Thiel, I.M. Sokolov, Scaled Brownian motion as a mean-field model for continuous-time random walks, Phys. Rev. E 89 (2014) 012115.
[19] L.R. Evangelista, E.K. Lenzi, An Introduction To Anomalous Diffusion and Relaxation, Springer, Berlin/Heidelberg, 2023.
[20] S. Kumar, D. Zeidan, Numerical study of Zika model as a mosquito-borne virus with nonsingular fractional derivative, Int. J. Biomath. 15 (2022) 2250018.
[21] S. Kumar, B. Ahmad, A new numerical study of space–time fractional advection-reaction–diffusion equation with Rabotnov fractional-exponential kernel, Numer. Methods Partial. Differ. Equ. 38 (2022) 457.
[22] R.R. Nigmatullin, Fractional integral and its physical interpretation, Theoret. Math. Phys. 90 (1992) 242.
[23] R. Hilfer, Applications of Fractional Calculus in Physics, World Scientific, Singapore, 2000.
[24] F. Mainardi, Fractional Calculus and Waves in Linear Viscoelasticity: An Introduction To Mathematical Models, World Scientific, Singapore, 2010.
[25] T. Sandev, Ž Tomovski, Fractional Equations and Models: Theory and Applications, Springer Nature, Cham, 2019.
[26] A.A. Kilbas, H.M. Srivastava, J.J. Trujillo, Theory and Applications of Fractional Differential Equations, Elsevier, Amsterdam, 2006.
[27] B.B. Mandelbrot, Fractals and Scaling in Finance: Discontinuity, Concentration, Risk. Selecta Volume E, Springer Science & Business Media, New York, 1997.
[28] S. Wei, W. Chen, J. Zhang, Time-fractional derivative model for chloride ions sub-diffusion in reinforced concrete, Eur. J. Env. Civ. Eng. 21 (2017) 319.
[29] H.G. Sun, Y. Zhang, W. Chen, D.M. Reeves, Use of a variable-index fractional-derivative model to capture transient dispersion in heterogeneous media, J. Contam. Hydrol. 157 (2014) 47.
[30] W. Cai, W. Chen, W. Xu, Fractional modeling of Pasternak-type viscoelastic foundation, Mech. Time-Depend. Mater. 21 (2017) 119.
[31] A.M. Mathai, R.K. Saxena, H.J. Haubold, The H-Function: Theory and Applications, Springer, New York, 2010.
[32] W.R. Schneider, W. Wyss, Fractional diffusion and wave equations, J. Math. Phys. 30 (1989) 134.
[33] K.B. Oldham, J. Spanier, The Fractional Calculus: Theory and Applications of Differentiation and Integration To Arbitrary Order, Academic Press, New York, 1974.
[34] K.S. Miller, B. Ross, An Introduction to the Fractional Calculus and Fractional Differential Equations, Wiley-Blackwell, New York, 1993.

[35] Q. Wei, W. Wang, H. Zhou, R. Metzler, A.V. Chechkin, Time-fractional Caputo derivative versus other integrodifferential operators in generalized Fokker–Planck and generalized Langevin equations, Phys. Rev. E 108 (2023) 024125.
[36] R. Metzler, E. Barkai, J. Klafter, Deriving fractional Fokker–Planck equations from a generalised master equation, Europhys. Lett. 46 (1999) 431.
[37] A.I. Rudenko, V.I. Arkhipov, Trap-controlled transient current injection in amorphous materials, J. Non-Cryst. Solids 30 (1978) 163.
[38] Z. Xiao, D. Yang, Y. Yuan, B. Yang, X. Liu, Fractal pore network simulation on the drying of porous media, Dry. Technol. 26 (2008) 651.
[39] E. Yarmola, P.P. Calabrese, A. Chrambach, G.H. Weiss, Interaction with the matrix: The dominant factor in macromolecular band spreading in gel electrophoresis, J. Phys. Chem. B 101 (1997) 2381.
[40] S. Redner, J. Koplik, D. Wilkinson, Hydrodynamic dispersion in a self-similar geometry, J. Phys. A: Math. Gen. 20 (1987) 1543.
[41] R. Hilfer, Threefold Introduction to Fractional Derivatives, in Anomalous Transport: Foundations and Applications, Wiley-VCH, 2008.
[42] H.M. Srivastava, Ž. Tomovski, Fractional calculus with an integral operator containing a generalized Mittag-Leffler function in the kernel, Appl. Math. Comput. 211 (2009) 198.
[43] Ž. Tomovski, R. Hilfer, H.M. Srivastava, Fractional and operational calculus with generalized fractional derivative operators and Mittag-Leffler type functions, Integr. Transf. Spec. F. 21 (2010) 797.
[44] T. Sandev, R. Metzler, Z. Tomovski, Fractional diffusion equation with a generalized Riemann–Liouville time fractional derivative, J. Phys. A: Math. Theor. 44 (2011) 255203.
[45] Ž. Tomovski, T. Sandev, R. Metzler, J. Dubbeldam, Generalized space–time FDE with composite fractional time derivative, Phys. A 391 (2012) 2527.
[46] R. Hilfer, Experimental evidence for fractional time evolution in glass forming materials, Chem. Phys. 284 (2002) 399.
[47] R. Hilfer, On fractional relaxation, Fractals 11 (2003) 251.
[48] T.R. Prabhakar, A singular integral equation with a generalized Mittag-Leffler function in the kernel, Yokohama Math. J. 19 (1971) 7.
[49] A.A. Kilbas, M. Saigo, R.K. Saxena, Generalized Mittag-Leffler function and generalized fractional calculus operators, Integr. Transf. Spec. F. 15 (2004) 31.
[50] R. Gorenflo, A.A. Kilbas, F. Mainardi, S.V. Rogosin, Mittag–Leffler Functions, Related Topics and Applications, Springer, Berlin, 2020.
[51] A.V. Chechkin, R. Gorenflo, I.M. Sokolov, Retarding subdiffusion and accelerating superdiffusion governed by distributed-order FDEs, Phys. Rev. E 66 (2002) 046129.
[52] A.V. Chechkin, R. Gorenflo, I.M. Sokolov, V. Yu. Gonchar, Distributed order FDE, Fract. Calc. Appl. Anal. 6 (2003) 259.
[53] T.A. Waigh, N. Korabel, Heterogeneous anomalous transport in cellular and molecular biology, Rep. Progr. Phys. 86 (2023) 126601.
[54] M. Balcerek, S. Thapa, K. Burnecki, H. Kantz, R. Metzler, A. Wyłomańska, A.V. Chechkin, Phys. Rev. Lett. 134 (2025) 197101.
[55] M. Balcerek, A. Wyłomańska, K. Burnecki, R. Metzler, D. Krapf, Modelling intermittent anomalous diffusion with switching fractional Brownian motion, New J. Phys. 25 (2023) 103031.
[56] V.M. Worlitzer, A. Jose, I. Grinberg, M. Bär, S. Heidenreich, A. Eldar, G. Ariel, A. Be'er, Biophysical aspects underlying the swarm to biofilm transition, Sci. Adv. 8 (2022) eabn8152.
[57] Y. Liang, S. Wang, W. Chen, Z. Zhou, R.L. Magin, A survey of models of ultraslow diffusion in heterogeneous materials, Appl. Mech. Rev. 71 (2019) 040802.
[58] S. Havlin, G.H. Weiss, A new class of long-tailed pausing time densities for the CTRW, J. Stat. Phys. 58 (1990) 1267.
[59] S. Denisov, H. Kantz, Continuous-time random walk with a superheavy-tailed distribution of waiting times, Phys. Rev. E 83 (2011) 041132.
[60] A. Bodrova, A.V. Chechkin, A.G. Cherstvy, R. Metzler, Ultraslow scaled Brownian motion, New J. Phys. 17 (2015) 063038.
[61] A. Bodrova, A.V. Chechkin, A.G. Cherstvy, H. Safdari, I.M. Sokolov, R. Metzler, Underdamped scaled Brownian motion: (non-)existence of the overdamped limit in anomalous diffusion, Sci. Rep. 6 (2016) 30520.
[62] A. Godec, A.V. Chechkin, E. Barkai, H. Kantz, R. Metzler, Localisation and universal fluctuations in ultraslow diffusion processes, J. Phys. A: Math. Theor. 47 (2014) 492002.
[63] A.V. Chechkin, J. Klafter, I.M. Sokolov, Fractional Fokker–Planck equation for ultraslow kinetics, Europhys. Lett. 63 (2003) 326.
[64] Y.G. Sinai, Theory Probab. Appl. 27 (1982) 256.
[65] G. Oshanin, A. Rosso, G. Schehr, Phys. Rev. Lett. 110 (2013) 100602.
[66] M. Caputo, Elasticitàe Dissipazione, Zanichelli Printer, Bologna, 1969.
[67] K. Diethelm, N.J. Ford, Numerical analysis for distributed-order differential equations, J. Comput. Appl. Math. 225 (2009) 96.
[68] T. Sandev, Ž. Tomovski, B. Crnkovic, Generalized distributed order diffusion equations with composite time fractional derivative, Comput. Math. Appl. 73 (2017) 1028.
[69] Ž. Tomovski, T. Sandev, Distributed-order wave equations with composite time fractional derivative, Int. J. Comput. Math. 95 (2018) 1100.
[70] T. Sandev, Ž. Tomovski, J.L.A. Dubbeldam, A.V. Chechkin, Generalized diffusion-wave equation with memory kernel, J. Phys. A: Math. Theor. 52 (2019) 015201.
[71] R. Garra, R. Gorenflo, F. Polito, Ž. Tomovski, Hilfer-Prabhakar derivatives and some applications, Appl. Math. Comp. 242 (2014) 576.
[72] Ž. Tomovski, J.L.A. Dubbeldam, J. Korbel, Applications of HP operator to option pricing financial model, Fract. Calc. Appl. Anal. 23 (2020) 996.
[73] I. Podlubny, Fractional Differential Equations, Academic Press, New York, 1999.
[74] S.G. Samko, A.A. Kilbas, O.I. Marichev, Fractional Integrals and Derivatives: Theory and Applications, Gordon and Breach Science Publishers, Yverdon, 1993.
[75] M. Caputo, Linear models of dissipation whose Q is almost frequency independent, Ann. Geophys. 19 (1966) 383.
[76] M. Caputo, Linear models of dissipation whose Q is almost frequency independent. II, Geophys. J. Int. 13 (1967) 529.
[77] T. Sandev, A.V. Chechkin, N. Korabel, H. Kantz, I.M. Sokolov, R. Metzler, Distributed-order diffusion equations and multifractality: Models and solutions, Phys. Rev. E 92 (2015) 042117.
[78] H.J. Haubold, A.M. Mathai, R.K. Saxena, Mittag-Leffler functions and their applications, J. Appl. Math. 2011 (2011) 298628.
[79] R. Garra, R. Gorenflo, F. Polito, Ž. Tomovski, Hilfer-Prabhakar derivatives and some applications, Appl. Math. Comput. 242 (2014) 576.
[80] W. Feller, An Introduction To Probability Theory and Its Applications, Wiley, New York, 1971.
[81] F. Mainardi, G. Pagnini, The wright functions as solutions of the time-FDE, Appl. Math. Comput. 141 (2003) 51.
[82] W.R. Schneider, W. Wyss, Fractional diffusion and wave equations, J. Math. Phys. 30 (1989) 134.
[83] A. Prudnikov, Y.A. Brychkov, O. Marichev, Integrals and Series, in: More Special Functions, vol. 3, Gordon and Breach, New York, 1990.
[84] E.W. Montroll, G.H. Weiss, Random walks on lattices. II, J. Math. Phys. 6 (1965) 167.
[85] J. Klafter, A. Blumen, M.F. Shlesinger, Stochastic pathway to anomalous diffusion, Phys. Rev. A 35 (1987) 3081.
[86] T. Sandev, A.V. Chechkin, H. Kantz, R. Metzler, Diffusion and Fokker–Planck-Smoluchowski equations with generalized memory kernel, Fract. Calc. Appl. Anal. 18 (2015) 1006.
[87] T.A.M. Langlands, Solution of a modified FDE, Phys. A 367 (2006) 136.
[88] M. Abramowitz, I.A. Stegun, Handbook of Mathematical Functions with Formulas, Graphs, and Mathematical Tables, Dover, New York, 1969.
[89] N. Korabel, G.D. Clemente, D. Han, F. Feldman, T.H. Millard, T.A. Waigh, Hemocytes in Drosophila melanogaster embryos move via heterogeneous anomalous diffusion, Commun. Phys. 5 (2022) 269.
[90] V.M. Worlitzer, A. Jose, I. Grinberg, M. Bär, S. Heidenreich, A. Eldar, G. Ariel, A. Be'er, Biophysical aspects underlying the swarm to biofilm transition, Sci. Adv. 8 (2022) eabn8152.

[91] S. Bo, L. Hubatsch, J. Bauermann, C.A. Weber, F. Jülicher, Stochastic dynamics of single molecules across phase boundaries, Phys. Rev. Res. 3 (2021) 043150.
[92] H.A. Shaban, R. Barth, L. Recoules, K. Bystricky, Hi-D: nanoscale mapping of nuclear dynamics in single living cells, Genome Biol. 21 (2020) 95.
[93] S. Kumar, Crank–Nicolson quasi-wavelet method for the numerical solution of variable-order time-space Riesz fractional reaction–diffusion equation, in: Applications of Fractional Calculus to Modeling in Dynamics and Chaos, 2022.
[94] C. Manzo, M.F. Garcia-Parajo, A review of progress in single particle tracking: from methods to biophysical insights, Rep. Progr. Phys. 78 (2015) 124601.
[95] D. Han, N. Korabel, R. Chen, M. Johnston, A. Gavrilova, V.J. Allan, S. Fedotov, T.A. Waigh, Deciphering anomalous heterogeneous intracellular transport with neural networks, eLife 9 (2020) e52224.
[96] M. Balcerek, A. Wyłomańska, K. Burnecki, R. Metzler, D. Krapf, Modelling intermittent anomalous diffusion with switching fractional Brownian motion, New J. Phys. 25 (2023) 103031.
[97] J. Ślęzak, R. Metzler, Minimal model of diffusion with time changing Hurst exponent, J. Phys. A: Math. Theor. 56 (2023) 35LT01.
[98] W. Wang, M. Balcerek, K. Burnecki, A.V. Chechkin, S. Janušonis, J. Ślęzak, T. Vojta, A. Wyłomańska, R. Metzler, Memory-multi-fractional Brownian motion with continuous correlations, Phys. Rev. Res. 5 (2023) L032025.
[99] M. Balcerek, K. Burnecki, S. Thapa, A. Wyłomańska, A.V. Chechkin, Fractional Brownian motion with random Hurst exponent: Accelerating diffusion and persistence transitions, Chaos 32 (2022) 093114.
[100] A. Pacheco Pozo, D. Krapf, Fractional Brownian motion with fluctuating diffusivities, Phys. Rev. E 110 (2024) 014105.
[101] M. Balcerek, S. Thapa, K. Burnecki, H. Kantz, R. Metzler, A. Wyłomańska, A.V. Chechkin, Multifractional Brownian motion with telegraphic, stochastically varying exponent, Phys. Rev. Lett. 134 (2025) 197101.
[102] R.L. Schilling, R. Song, Z. Vondracek, Bernstein Functions, De Gruyter, Boston, 2010.